AN INVESTIGATION TO SEISMIC INDUCED SOIL PRESSURES ON RELATIVELY RIGID STRUCTURES WITH DEEP EMBEDMENT

By

Weihang (Norman) Dong, B. Eng.

A Project Report Submitted to the School of Graduate Studies

in Partial Fulfilment of the Requirements for the Degree of

MASTER OF ENGINEERING

Department of Civil Engineering

McMaster University, Hamilton, Ontario, Canada

McMaster
University

MASTER OF ENGINEERING (2010)   McMaster University

(Civil Engineering)   Hamilton, Ontario

TITLE: An investigation to seismic induced soil pressures on relatively rigid structures with deep embedment

AUTHOR: Weihang (Norman) Dong

                   B. Eng. (Northeastern University)

SUPERVISOR: Dr. Peijun Guo

NUMBER OF PAGES: xv, 136

ABSTRACT

Design of earthquake-resistant structures has been an important area in both research and engineering practice for decades. Realistic determination of seismic loading on structures is one of the governing design criteria for design of new buildings or evaluation of existing structures. For the nuclear industry, the performance of structures is extremely important owing to public safety concerns.

This report explores the methodologies used to calculate seismic-induced soil pressure applied onto partially embedded structures. A critical review was performed on different methods developed in the past, which includes simplified analytical approaches based on either yielding wall theory or rigid wall theory and detailed dynamic analysis with the consideration of soil-structure interaction effects. Assumptions, range for appropriate application, and corresponding shortcomings of these methods are identified. Several critical issues that have significant impact on the soil-structural response but are not sufficiently taken into account in most existing models, are identified. These include embedment effects, interface boundary conditions and material nonlinearity. Following the review, a detailed seismic analysis using the finite element method is carried out to explore the effects of embedment effects, interface boundary conditions and material nonlinearity on seismic earth pressure. A simplified CANDU 6 reactor building excited by an artificial strong ground motion is used in this analysis. The seismic earth pressures obtained from this detailed seismic analyses under various conditions are then compared with the simplified approaches to evaluate their accuracy.

This report is organized as follows. After an introduction on the background and the scope of this study, a review on the regulations relevant to seismic soil-structure interaction and the determination of seismic earth pressure in different codes and regulatory guidelines is presented in Chapter 2, followed by a critical review specifically on existing methods to determine the seismic earth pressure, is presented in Chapter 3. Chapter 4 establishes a finite element model for a simplified CANDU 6 reactor building for detailed seismic analysis. The factors investigated include material properties, boundary conditions and the input for ground motion. Chapter 5 provides detailed analysis and comparisons of results obtained from the finite element seismic analysis and the simplified approaches. The major finding and conclusions from this study are summarized in Chapter 6, with some recommendations being made.

The information and conclusions presented in this report can be generally used as a design reference, or a starting point for continues studying on this particular topic for future design of nuclear facilities.

DEDICATION

I want to dedicate this report to my family: to my wife, Nan Kou, for her constant support and encouragement on my career development, and to my son Alex for bringing so much happiness to my life.

I also wish to express my sincere appreciations to my supervisor, Dr. Peijun Guo, offering me the opportunity to continue my education, and thank him for his great help, advice and guidance to complete my Master program.

Finally, I want to thank Mr. Robert Kloosterhuis who helped with editing to make this report readable and professional.

TABLE OF CONTENTS

LIST OF FIGURES

LIST OF TABLES

LIST OF SYMBOLS

A	Constant spectral acceleration of soil
C_v	Force coefficient as a function of Poisson's ratio of the soil medium
$[C]$	Damping matrix of the structural system
D	Constant spectral displacement of soil
f_0	Frequency of harmonic motion
f_s	Soil column frequency
f_L, f_U	Lower and upper bound frequencies corresponding to constant spectral velocity
f_c'	Specified compressive strength of concrete
E_c, E_s	Elastic modulus of concrete and soil, respectively
F	Inertial force of the superstructure
F_a	Acceleration-based site coefficient
F_x, F_y	Components of body forces per unit volume in x and y direction
F_{Total}	Total lateral seismic force
G	Shear modulus of the soil
H	Thickness of soil layer; Wall height; Embedment depth
I_E	Seismic important factor as per NBCC2005
k_h, k_v	Horizontal and vertical ground acceleration coefficient, respectively
K_{AE}	Coefficient of active earth pressure
K'_{AE}	Transformed coefficient of active earth pressure
K_{PE}	Coefficient of passive earth pressure

$[K]$	Stiffness matrix of the structural system
L	Length of yielded soil wedge; Horizontal distance between two rigid boundaries; Building width
m	Total soil mass
$[M]$	Mass matrix of the structural system
p_y	Distribution function of lateral earth pressure as per Ostadan
P	Total dynamic earth pressure
P_a, P_p	Total active and passive soil pressure, respectively
P_A	Static component of total soil pressure
Q	Total dynamic thrust force
ΔP_{AE}	Dynamic component of total soil pressure
S_a	Acceleration spectral amplitude of the soil's free-field response
$S_a(0.2)$	Spectral response acceleration for a structure's period equal or less than 0.2 s
$S(T)$	Design spectral acceleration
T	Period of propagating shear wave or primary wave
T_{soil}	Fundamental period of soil layer
$\ddot{u}_g$	Ground acceleration
$\{U_b\}$	Displacement vector of the structural system under a unit displacement in the motion direction
V	Constant spectral velocity of soil
V_d	Soil dilatational wave velocity
V_P	Soil primary wave velocity
V_S	Soil shear wave velocity
V_{SD}	Shear wave velocity of the bedrock
V_{SE}	Mean shear wave velocity of the surrounding soil
W	Weight of soil wedge
$\{X\}$	Column vector of relative displacements

$\{\dot{X}\}$	Column vector of relative velocities
$\{\ddot{X}\}$	Column vector of relative accelerations
β	Slope inclination of the ground surface behind the wall; Shear ratio of surrounding soil
β_c, β_s	Critical damping of concrete and soil, respectively
δ	Frictional angle at the interface of the wall and backfill
ϕ	Internal soil friction angle
ϕ_{peak}	Peak soil friction angle at initial active failure
ϕ_{res}	Residual soil friction angle at secondary active failure
γ	Unit weight of the backfill soil
γ_c, γ_s	Unit weight of concrete and soil, respectively
λ	Soil's damping ratio; Wavelength of vertically propagating shear wave
η	Wavelength of vertically propagating primary wave
ν	Soil's Poisson's ratio
ν_c, ν_s	Poisson's ratio of concrete and soil, respectively
θ	Seismic inertial angle relative to the gravity direction
ρ	Soil density
σ_x, σ_y	Normal stresses in x and y direction, respectively
τ_{xy}	Shear stresses in the soil
ω	Base acceleration frequency of the earthquake motion
ω_{11}	Fundamental frequency of the wall-soil system
ψ	Inclination angle at the contact surface of the structure
Ψ_ν	Adjustable factor corresponding to different soil's Poisson's ratio

ABBREVIATIONS

ACR Advanced CANDU Reactor

AECL Atomic Energy of Canada Limited

AIJ Architectural Institute of Japan

ASCE American Society of Civil Engineers

BEM Boundary Element Method

BWR Boiling Water Reactor

CANDU Canada Deuterium Uranium

CFR Code of Federal Regulations

CNSC Canadian Nuclear Safety Commission

CSA Canadian Standards Association

DBE Design Basis Earthquake

DGM Design Ground Motion

DOF Degree of Freedom

DP Drucker-Prager

EPRI Electric Power Research Institute

FEM Finite Element Method

FEMA Federal Emergency Management Agency

GDE Generic Design Earthquake

GRS Ground Response Spectra

IAEA International Atomic Energy Agency

ISSC International Seismic Safety Center

JEA Japan Electric Association

LSST Large Scale Seismic Test

MDOF	Multi-Degree of Freedom
M-O	Mononobe-Okabe
NBCC	National Building Code of Canada
NEHRP	National Earthquake Hazards Reduction Program
NMPC	Niagara Mohawk Power Corporation
NMPP	Nine Mile Point Plant
NPP	Nuclear Power Plant
NRC	US Nuclear Regulatory Commission
NURGE	Nuclear Regulatory
OBE	Operational Basis Earthquake
PBMR	Pebble Bed Modular Reactor
PDE	Partial Differential Equation
PGA	Peak Ground Acceleration
PGD	Peak Ground Displacement
PGV	Peak Ground Velocity
PWR	Pressurized Water Reactor
RG	Regulatory Guide
SASSI	A System for the Analysis of Soil-Structural Interaction
SDE	Site Design Earthquake
SDOF	Single Degree of Freedom
SMR	Small Modular Reactor
SR	Sway and Rocking
SRP	Standard Review Plan
SSC	Structure, System and Component
SSE	Safe Shutdown Earthquake
SSI	Soil-Structural Interaction
TPC	Taiwan Power Company

1 INTRODUCTION

1.1 BACKGROUND AND MOTIVATIONS

Earthquake engineering is an interesting topic for both engineers and researchers. Seismic loading is one of the governing design criteria when designing a new building or evaluating an existing structure, especially in the nuclear engineering field. This is mainly due to public safety concerns. Conventional structural design methods utilize equivalent static analysis or simple dynamic analysis, and neglect the effects of soil-structural interaction (SSI). Although this may be acceptable and practical for structures on shallow foundations resting on relatively stiff soil, the effects of SSI become prominent for deeper embedded heavy structures such as the reactor building in nuclear power plants (NPP).

Research on SSI has been carried out over the past few decades. Considerable has been made with regard to understanding the working mechanisms and behaviors between the structure and soil media, particularly when subjected to an earthquake strike. The impact of SSI on the seismic response of structures has been proven by both theoretical analyses and abundant testing data. Severe structural damages encountered in previous earthquake events, such as the 1995 Kobe earthquake and the 1989 Loma Prieta earthquake, have highlighted that a structure's seismic behavior is highly influenced not only by the response of the superstructure, but also by the response of the foundation and

ground as well. In addition, the requirements of performance-based design dictate that the integration of the structure and soil can provide more reliable and economic designs than when the SSI is not taken into account. Hence, almost all current regulatory codes and standards around the world recommend considering overall system response when performing structural analysis for nuclear safety-related structures.

With the development of third generation NPPs, there is a tendency to deeply embed the containment buildings and safety-related structures. Even some special designed small units (e.g. Small Modular Reactor [SMR], Pebble Bed Modular Reactor [PBMR], etc.) are fully hidden below the grade (Xu [2005]), which benefits the operating process and addresses safety concerns. However, most of currently available codes and standards in use, especially in Canada, were initialized more than ten years ago for last-generation NPPs, which are mostly near surface, shallow embedded structures. The analysis methodologies recommended in these codes utilize the bonded soil-structure models, which are still widely in use in the nuclear energy industry, even though it may not adequately describe the behavior of deeply embedded structures subjected to seismic loading. For example, when increasing embedded depths under the consideration of SSI effects, kinematic interaction between structures and the surrounding soil tends to gradually supersede initial interaction. At the same time, the seismic soil pressure on the basement perimeter walls of the underground structure becomes more important. From regulatory and application points of view, these potential seismic issues for a NPP safety related structure with deeper embedment should be carefully addressed and investigated when starting a new design.

It is worth mentioning that most research effort and interest on SSI focus on the study of input ground motions and the corresponding structural seismic response. Relatively limited research has been carried out on how to quantify the seismic-induced soil pressures on underground structures, using either equivalent static analysis or numerical dynamic analysis. It is generally agreed that equivalent static analysis cannot provide in-depth results for the performance of structures under seismic loading. Virtues of fast computer science development have made performing a complex dynamic finite element (FE) analysis with the help of numerical modeling engines (i.e., SASSI, Dyna3D, Stardyne, LS-Dyna, ANSYS, etc.) affordable. However, owing to its simplicity, traditional equivalent static analysis techniques are still widely in use in engineering design, particularly during the preliminary design phase, or when performing independent peer review and design verification.

The main goal of this report is to explore fundamental code and regulatory requirements applied to deeply embedded structures, and to investigate the prevalent analysis methodologies available in practice or based on state-of-the-art studies to predict and quantify soil pressures induced by earthquakes. The report also provides a general comparison and assessment through a sample case to verify if these available analysis methods are capable and adequate to capture seismic behavior. The information presented herein can be generally used as a design reference, and demonstrates the necessity to continue studying the topic for future designs of nuclear facilities.

The following issues and concerns, which can have significant impact on the analysis of seismic-induced soil pressures on embedded structures, form the principle parts of the report:

1. The regulatory requirements;

2. The availability of analysis methodologies including both static and dynamic analysis;

3. The accuracy of available equivalent static analysis methods;

4. The effect of embedment depth on the structural response under the strong ground motions;

5. The application of SSI when performing dynamic analysis;

6. The relation between the kinematic interaction and the inertial interaction;

7. The linear and nonlinear contact behavior at the soil and structure interfaces;

8. The effects of non-linear characteristic of soil material;

9. The possibility to simplify the analysis process.

Although the study is trying to broadly contain typical design issues and concerns, there are still many factors and variables required for conducting detailed analysis, but conditioned as assumptions and not fully addressed in the report. In the case of conflicts with codes or specific concerns not included, further analysis shall be considered and incorporated by the individual responsible engineer for particular project following more

restrict criteria and requirements. Modifications and adjustments are deemed necessary based on further study and investigation.

The report is organized in six chapters. Following Chapter 1 that presents a general introduction and a brief background description about the project, Chapters 2 and 3 provide a comprehensive literature review on existing codes/standards in practice as well as available methods to determine seismic-induced soil pressures. A case study on a simplified CANDU reactor building is described in Chapter 4, which also provides a description on the associated analysis models, necessary assumptions and inputs applicable to this case study. Chapter 5 incorporates and applies all methods as discussed in Chapter 3, and provides detail discussions and comparisons on the computation results to evaluate and verify if these discussed methods can reasonably predict seismic responses and adequately quantify soil pressures under strong ground motions. Finally, Chapter 6 summarizes conclusions and recommendations to identify how various analytical methods commonly utilized in practice are capable and acceptable to extend their application assisting the future design and development of new NPP facilities.

2 CODE AND REGULATORY REVIEW

This chapter presents a literature on existing codes/standards in practice, as well as the recommended methods to determine seismic-induced soil pressures.

The nuclear reactor building is part of the containment system and is defined as a safety related structure. Its function is to limit the release of radioactive material to the environment during both normal operation condition and during (or after) extreme environmental or accidental conditions. Owing to safety concerns, the reactor building must be designed following very stringent requirements, as reflected in codes, standards and regulatory guidelines published in Canada, US, Japan & IAEA. This section provides a review focusing on the applicability and limitations of the methods to determine seismic-induced soil pressures as recommended in these codes and standards. The major aspects addressed by the regulatory and code reviews include:

1. Determination of free field ground motion;

2. Methodologies recommended by regulations and used for practices;

3. Requirements for considering SSI to predict the seismic response;

4. Assessment of seismic-induced soil pressures applied to the embedded structures; and

5. Fundamental design criteria used for seismic design and analysis.

6

2.1   CANADIAN CODE REQUIREMENTS

2.1.1   National Building Code of Canada (NBCC 2005)

NBCC 2005 defines the design ground motion (DGM) having a 0.04% annual probability of exceedance at a median confidence level. Utilizing dynamic analysis to simulate the seismic effects is highly recommended by the building code. The equivalent static force procedure is only applicable for certain simple cases under strict conditions. NBCC specifies the seismic hazard in terms of spectral response acceleration, which is used to determine the minimum lateral seismic force. The code notices and requires incorporating the amplification effects on the ground motions due to different soil damping values. By assuming the elasticity, the fundamental period of the soil layer can be estimated as $T_{soil} = 4H / V_S$, in which, H is the thickness of soil layer, and V_S represents the shear wave velocity.

As specified in NBCC 2005 Section 4.1.8.16 (4), for moderate to high seismicity region where its design spectral acceleration $S(T)$ is greater than 0.35, the basement walls shall be designed to resist increased lateral soil pressures due to the movement of backfill or natural ground associated with earthquake ground motions. The regional design spectral acceleration can be determined as $S(T) = I_E F_a S_a(0.2)$, in which, I_E is the seismic important factor, F_a is acceleration-based site coefficient, and $S_a(0.2)$ represents the 5% damped spectral response acceleration for a period equal or less than 0.2 s. In NBCC 2005 Commentary J, the method based on Mononobe-Okabe theory (Mononobe and Matsuo [1929], Okabe [1926]) is recommended. However, considering that the

basement walls actually have "non-yielding" or non-sliding characteristics, the required movement in Mononobe-Okabe theory may not be sufficient to develop active earth pressures. The concern regarding dynamic forces acting on a non-yielding (non-sliding) wall on a rigid base needs to be properly addressed and incorporated into the design and analysis.

2.1.2 Canadian Standards Association (CSA)

The CAN/CSA-N289 Standard series deal with the seismic qualification process for Canadian CANDU reactors, which utilize pressurized heavy water technology developed by AECL. The N289 Standard series were initially developed in the 1980s for last generation CANDU reactors, but are reviewed and reaffirmed periodically with minor amendments over the years. They are currently under significant revision and development for new generation of ACR-1000 nuclear power plants (NPP) that takes into consideration of more rational and modern engineering knowledge.

CSA/CAN-N289.1 describes the seismic design philosophy for NPP structures, and specifies the seismic classifications as three different magnitudes, which are Design Basis Earthquake (DBE), Site Design Earthquake (SDE), and Generic Design Earthquake (GDE). In accordance with N289.1, all safety related structures or systems (e.g., reactor buildings) must be seismically qualified to DBE level earthquakes to demonstrate the structure or component's ability to perform their safety function during and/or after the time it is subjected to forces resulting from one DBE, which represents most potentially severe earthquake ground motions under a probability of 1×10^{-4} per annum exceedance

during the lifetime of the plant. Methodologies commonly used and recommended for seismic qualifications are through structural analysis as per N289.3 or by testing following N289.4.

N298.3 describes the ground response spectra and ground motion time-histories to be used for the seismic qualification. The development of engineering design ground response spectra is specified in Section 3.2 based on standard amplification factors (Table 1) and anchored to a peak ground acceleration determined by the seismic hazard assessment. N289.2 outlines the procedure and methodology used to determine the design seismic ground motions. AECL is proposing to adjust the peak seismic ground motion parameters to 0.3g (acceleration), 213.3 mm/sec (velocity) and 93.2 mm (displacement) to account for most critical scenarios based on current research and recent development. The constant velocity value extends from the lower bound frequency f_L to the upper bound frequency f_U, which are determined as

$$f_L = \frac{V}{2\pi D}, \quad f_U = \frac{A}{2\pi V}$$

where A, V and D represent constant spectral acceleration, velocity and displacement, respectively. Accordingly, the normalized ground response spectra for rock sites are developed, as summarized in

Table 2.

A series of the ground response spectra with regard to different damping values are plotted in Figure 2-1, which will be used as seismic inputs in this study when performing dynamic analysis in Chapter 4.

Table 1: Amplification Factors for Developing Ground Response Spectra

Damping Ratio (%)	Lower Frequency Range	Intermediate Frequency Range	Upper Frequency Range
0.0	3.59	4.48	5.83
0.5	3.24	3.95	4.98
1.0	3.04	3.64	4.52
2.0	2.74	3.23	3.90
3.0	2.53	2.93	3.48
5.0	2.23	2.52	2.92
7.0	2.00	2.25	2.56
10.0	1.76	1.94	2.18
20.0	1.32	1.42	1.52

Table 2: Seismic Ground Response Spectra for Rock Sites

Damping Ratio (%)	Lower Frequency Range	Intermediate Frequency Range	Upper Frequency Range
	Displacement (mm)	Velocity (mm/sec.)	Acceleration (% of g)
0.0	334.6	955.6	174.9
0.5	302.0	842.5	149.4
1.0	283.3	776.4	135.6
2.0	255.4	689.0	117.0
3.0	235.8	625.0	104.4

5.0	207.8	537.5	87.6
7.0	186.4	479.9	76.8
10.0	164.0	413.8	65.4
20.0	123.0	302.9	45.6
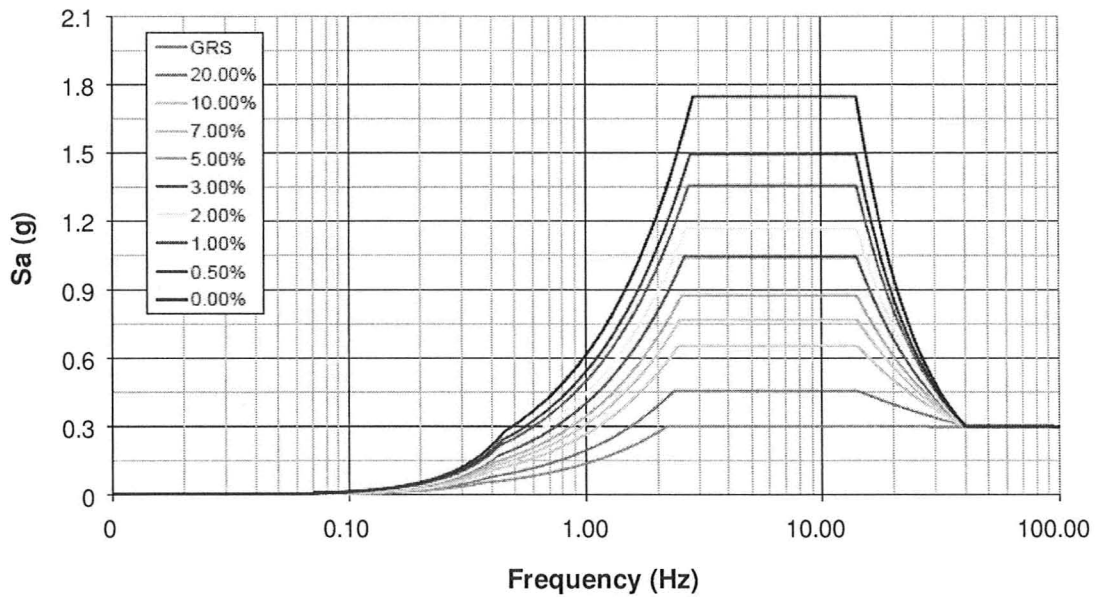
Figure 2-1: Response Spectra for Rock Sites

In accordance with N289.3, the input spectra shall be applied in three orthogonal directions independently and simultaneously, and the peak vertical ground motion parameters shall be taken as 2/3 of the horizontal motion parameters.

N289.3 requires considering the dynamic characteristic of structural response when performing the seismic qualification analysis. The acceptable methods and procedures for performing a dynamic analysis are outlined in Chapter 4. Two analytical techniques (namely, the complete interaction technique and the substructure technique) commonly used to incorporate the effects of SSI are discussed and permitted by the

standard. In these two techniques, the complete interaction technique represents the structure and the surrounding soil in one dynamic model with qualified seismic input motion, reasonable boundary and interface conditions. In contrast, the substructure technique deals with the soil and the structure separately, with the soil-structure interface be simplified as soil springs and dash pots. The spring constants and damping values at the soil-structure interface are first determined by FE analysis for soil first and then applied as boundary conditions onto the standalone structure for the dynamic structural modeling, which can be carried out using either the finite element method (FEM) or the lumped-mass-spring method. The FEM is particularly recommended for structures with deep embedment. In addition, N289.3 emphasizes the importance of the variation in soil properties by requiring that the soil's non-linear characteristic shall be properly addressed and incorporated into the dynamic analysis.

N289.3 requires that seismic-induced lateral earth pressure applied onto embedded portions of structures shall be taken into account. As described in Section 4.3 of N289.3, although a dynamic analysis using FEM should be performed to obtain the dynamic pressure, an equivalent-static analysis method may be used to simplify the analysis process. However, an appropriate factor against uncertainties shall be adequately evaluated to ensure that a conservative result is derived accordingly.

2.2 US CODE REQUIREMENTS

2.2.1 US Nuclear Regulatory Commission (NRC)

The US NRC represents the US government for regulating the operation of commercial nuclear power plants (NPP) through licensing, inspection and enforcement of its regulatory requirements. The most important NRC regulation documents to guide nuclear facilities design are Federal Regulations 10 CFR 100 Appendix A and 10 CFR 50 Appendix A & B. These documents provide design criteria that have the weight of federal law requiring compliance.

10 CFR 50 Appendix A sets forth the general design criteria used in safety-class nuclear plant facilities design. Criterion 4 defines the environmental design bases. 10 CFR 100 Appendix A defines the Operational Basis Earthquake (OBE), Safe Shutdown Earthquake (SSE) and the manner to determine their intensities. The CFR recommends using a suitable dynamic analysis or a suitable qualification test to demonstrate the capability of safety related structures to withstand a SSE and other concurrent loads. It is required that the dynamic analysis shall take into account soil-structure interaction effects and the expected duration of vibratory motion. Except where it can be demonstrated, an equivalent static load method may be used only when it can be shown that such a method provides adequate conservatism.

In addition, NRC Regulatory Guide (RG) 1.60 describes procedures to determine SSE design response spectra corresponding to the expected maximum ground accelerations, specifically for design purposes. Different than CSA standards, RG 1.60

specifies that the vertical component is two third (2/3) or one (1) time the value of the horizontal design response spectra for frequencies less than 0.25 cps or higher than 3.5 cps, respectively, while the ratio varies between two third (2/3) or one (1) for frequencies in between. The critical damping intended for elastic dynamic seismic analysis is specified in RG-1.61.

NRC Standard Review Plan (NUREG-0800) provides generic discussions and guidelines regarding seismic analysis related issues to be incorporated into the structural design, including Section 3.7.1 for the selection of seismic design parameters, Section 3.7.2 for performing seismic system analysis, and Section 3.8.5 for foundation design.

Standard Review Plan (SRP) Section 3.7.2 describes methods and criteria for performing equivalent static or dynamic seismic analysis. These criteria include consideration for SSI effects and the combination of three orthogonal earthquake motions when performing a dynamic analysis. The seismic response of structures can be determined using a direct approach method (simultaneous solutions with the free field and the structure) or a substructure approach method (combined with separate solutions) in accordance with SRP Section 3.7.2.

A complete SSI analysis model is recommended to properly account for the variation of strain-dependent soil properties (e.g., damping, shear modulus, etc.), the contact behavior at the interface of the soil and structure, the effects due to the kinematic and inertial interaction for superstructure and sub-structure, the effect of pore water on structural responses, etc. Factors that should be considered and incorporated in a SSI

analysis include: (1) the extent of embedment (2) the layering of soil/rock strata and (3) the boundary of soil-structure model. If a nonlinear analysis is performed, the results of the nonlinear analysis should be interpreted on the basis of the linear or equivalent linear analysis in according to SRP Section 3.7.2. Alternatively, the soil nonlinearity can be simplified using equivalent linear soil material properties determined from an iterative linear approach.

Except for Section 3.8.5, in which the method to determine dynamic soil pressure in foundation design is described, the Standard Review Plan (SRP) does not have any particular sections to regulate or guide the design of deeply embedded or fully buried structures. However, the SRP implies that the linear elastic model used to evaluate SSI effects is capable of conservatively calculating seismic soil pressures applied onto the basement perimeter walls. It is expected that the SRP should provide detail discussions on how to evaluate the dynamic soil pressures based on the feedbacks of research and experience, and then recommend an alternative analysis method (e.g., non-linear models) to produce results that are more accurate and close to reality.

2.2.2 American Society of Civil Engineers (ASCE)

Similar to CSA standards, ASCE standards provide technical guidelines for promoting safety, reliability, productivity and efficiency across all areas of civil engineering. The standards relevant to nuclear facilities include ASCE 4-98 and ASCE 43-05, which are consensus documents to provide minimum requirements and design criteria as well as acceptable methods for seismic analysis and design of safety-related

structures in a nuclear facility. These standards specify that the seismic responses shall have about a 90% chance of not being exceeded for an input response spectrum specified at the 84th percentile non-exceedance level.

Section 3.1 of ASCE 43-05 stipulates that seismic demand shall be computed in accordance to ASCE Standard 4 requirements, and allows use of different methods including linear equivalent static analysis, linear dynamic analysis, nonlinear analysis and complex frequency response methods. Most analysis methods described in ASCE 4-98 are consistent with the methods given in NRC regulatory guidance documents.

ASCE 4-05 Section 2.0 describes the seismic ground motion inputs used for a dynamic analysis. The seismic ground motions are specified by smoothed response spectra conservatively to account for uncertainties in future earthquake motions. Similar to CSA N289, the design ground motions are defined in terms of peak ground acceleration (PGA), peak ground velocity (PGV), and peak ground displacement (PGD). The seismic inputs shall be applied simultaneously in three orthogonal directions whose vertical component is adjusted to two-third (2/3) of the corresponding horizontal components throughout the entire frequency range. Figure 2-2 presents a plot of the 5% damped spectrum, which is scaled by a median amplification factor to 0.3 g PGA at the surface of a soil site.

General guidance for modeling a NPP structure is provided in Section 3.1 of ASCE Standard 4, including general requirements, how to develop horizontal and vertical motions, multistep and one-step analysis methods, FE discretization considerations,

selection of material properties, dynamic coupling criteria, methods to determine stiffness, mass and damping. Either Rayleigh damping or composite damping can be used in the analysis. In general, Rayleigh damping is suitable for structures composed of the same material or with similar damping characteristics. The composite damping is used to accommodate different damping properties of individual sub-structures within the whole structural system.
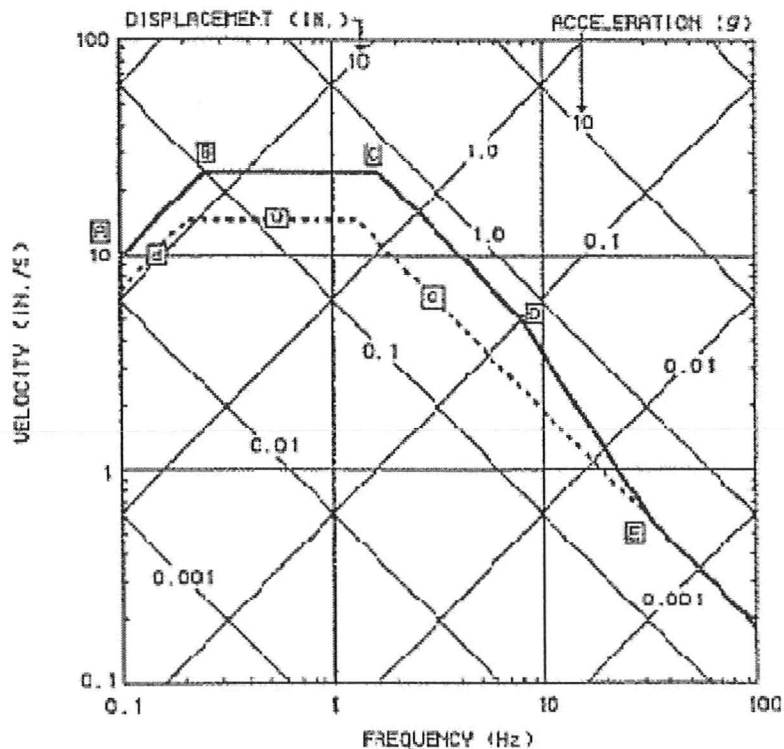
Figure 2-2: Response Spectra Scaled to 0.3 PGA for 5% Damping Soil Sites

Section 3.2 of ASCE standard 4 describes, in detail, the methods for structural seismic analysis, which include the time-history method, the response spectrum method, the complex frequency response method, and the equivalent-static method. Also, seismic dynamic responses can be analyzed by either linear or nonlinear methods. The basic equation of motion for linear system is given as

$$[M]\{\ddot{X}\}+[C]\{\dot{X}\}+[K]\{X\}=-[M]\{U_b\}\ddot{u}_g \qquad \text{Eq. (1)}$$

where, $[M]$, $[C]$ and $[K]$ represent the system's mass matrix, damping matrix and stiffness matrix, respectively; $\{X\}$, $\{\dot{X}\}$ and $\{\ddot{X}\}$ represent the column vector of relative displacements, velocities and accelerations, respectively; $\{U_b\}$ is the displacement vector of the structural system under a unit displacement in the motion direction, and $\ddot{u}_g$ represents the ground acceleration.

When the response spectrum method is used, the above equation can be uncoupled using the linear coordinate transformer and then superposing sufficient number of participated modes. It is noted that the response spectrum method is not suitable for nonlinear multi-degree-of-freedom (MDOF) systems because the superposition of modes is no longer valid. On the other hand, the use of nonlinear analytical methods is the basis of earthquake design criteria in codes for critical facilities. When performing nonlinear analysis, both geometric and material nonlinearities shall be considered. Usually, nonlinear soil behavior is simplified by equivalent linearization techniques, which iterate

on the linear material properties to converge on a measure associated with the strain level over the duration of the excitation.

The requirements for SSI modeling are given in Section 3.3 of ASCE Standard 4. Variations of free-field motion for an SSI analysis can be determined by incorporating vertically propagating shear and compression waves into a linear elastic soil model. It should be noted that torsional effects caused by the eccentricity of mass centre and rigidity center, as well as accidental eccentricity may induce significant impacts on embedded structures.

According to ASCE Standard 4, two methods are generally used for SSI analysis: (a) the direct method, which develops a combined soil-structure model solved by the FE approach, and (b) the impedance method, which separates the free field from the structure. In general, the impedance approach is limited to linear or equivalent linear problems, while the direct method is applicable to modeling both linear and nonlinear material behaviors.

A SSI analysis by the direct method requires locating soil boundaries far away from the structure to minimize the reflection effects from the artificial boundaries, which may have significant influence on the seismic response of the structures. The location of the boundaries is a function of frequency and soil damping, and is usually taken at four or five effective radii from the edge of the foundation. Either elementary or viscous boundary can be used for the SSI analysis. An elementary boundary may be fixed, free, or a combination. On a viscous boundary, the viscous dashpots oriented normal and

tangential to the lateral boundary are placed. The difference between the elementary and viscous boundaries is that the dashpots on the viscous boundaries act on the relative motion of the soil-structure system with respect to the free-field motion and absorb energy of incident waves.

The impedance approach, on the other hand, decomposes the SSI problem into a series of simpler problems, each being solved independently and the results being superimposed over each other to obtain the response of the whole system. The analysis generally consists of three steps: (1) determination of the input motion of foundation (kinematic interaction problem), (2) determination of foundation stiffness or impedance functions (inertial interaction problem), and (3) analysis of the coupled soil-structure system by solving equations of motion. The effect of embedment, which may be neglected for shallow foundations with depth to width ratio less than 0.3, could be significant for deeply embedded structures. Even though the standard does not specify any accurate or rigorous analytical solutions for deep embedment, it has been noted that during a strong earthquake strike potential soil-structure separation may occur, which could reduce the effectiveness of embedment. In order to account for embedment effects in a SSI analysis properly, it is recommended the connection between structure and soil beyond the upper half of the embedment should be separated in any analysis.

An equivalent linear elastic approach is recommended by ASCE-4 using a direct FE method to determine the dynamic soil pressures on an earth-retaining structure. However, it is assumed that the soil-structure connectivity is well maintained over the entire embedment height. The coefficient of friction at the interface can be set as either

zero or infinite. Adjustment to the soil properties may be required to adequately reflect the influence of strain level developed in soil. An equivalent static analysis proposed by Wood (1973) can be used to conservatively calculate the dynamic soil pressure as an alternative to a FE analysis.

When displacements required to develop the active earth pressure can be tolerated without compromising the wall's functionality, the Mononobe-Okabe (M-O) approach is acceptable to estimate seismic soil pressures. The approximate magnitude of these displacements is about 0.1% of the wall height for cohesionless backfills. The calculated resultant dynamic force shall be applied at 0.6 of the soil embedment height measured from the bottom. Considering the potential separation near the ground surface, the relieved earth pressure could be transferred further down, which could result in higher wall pressures at deep depths. This in turn would change the distribution of soil pressures and the corresponding loading center.

It is obvious that neither elastic nor active earth pressure solutions are suitable for the case in which potential separation may happen between the soil and structure. As such, a non-linear FE analysis model shall be used in this study to further simulate the actual contact response between the soil and structure to obtain more reliable seismic soil pressures on the structure. It is not clear how conservative or reliable elastic or active earth pressure solutions in estimating seismic soil pressures. Further investigation is necessary to avoid any unacceptable underestimation when performing the designs for a NPP safety related structure using these methods.

2.3 JAPANESE CODE REQUIREMENTS

The seismic design methods applied for Japanese nuclear power plants (NPP) is regulated by JEAG 4601-1987, which is published by Japan Electric Association (JEA) and used as the guideline for the structural analysis and design of nuclear power plants in Japan.

In the Japanese nuclear industry, design basis earthquakes are classified into two categories: the extreme design earthquake (S1) and the maximum design earthquake (S2). The input seismic ground motions are developed based on the data from previous earthquake experience, empirical testing, and research studies. JEAG 4601 allows for both conventional analysis method and FE method to evaluate seismic effects applied on an embedded structure's sidewall.

JEAG 4601, which requires SSI effects be incorporated in the analysis by using simplified or detailed approaches, discusses several practical methods and their limitations for SSI analysis. By recognizing the uncertainties associated with these SSI analysis methods, JEAG 4601 simplifies and standardizes the analysis models by proper selection of element sizes and treatment of boundary conditions. These simplified approaches include the sway and rocking (SR) model, ground compliance theory, and vibration admittance theory.

Among detailed SSI approaches, the empirical SR model and multi-degree-of-freedom (MDOF) parallel ground model are mostly applied in Japan. These are described in detail in JEAG 4601. Only the MDOF parallel soil model and FEM methods are applicable to accommodate embedment effects. Limitations regarding the contact behavior in both FE models and the linear approaches are identified and discussed in the supplement of JEAG 4601. The 1991 Supplement also summarizes different methods used to determine earth pressure on underground walls based on recorded pressure data and analyses. The long-term earth pressure is evaluated by taking into account the effects of excavation, building construction and backfill properties. Methods to determine the seismic earth pressure during earthquakes (including the simplified approach based on SSI) and their limitations are also described in the Supplement.

2.4　IAEA CODE REQUIREMENTS

The IAEA is an international organization that seeks to promote peaceful uses of nuclear energy. To enhance the sharing of information and experience among IAEA Member States concerning seismic safety at nuclear facilities, in 2008 the IAEA established the International Seismic Safety Center (ISSC), which develops safety standards and provides interpretation for their application related to site selection, site evaluation and seismic design.

IAEA NS-G-1.6 & NS-G-3.6 recommend a similar approach for predicting seismic motion and for analysis. Most of their design criteria and recommended analysis methodologies are similar to ASCE and CSA standards.

3 METHODS TO DETERMINE SEISMIC EARTH PRESSURE

3.1 INTRODUCTION

Determination of ground-seismic-motion-induced soil pressures is an important topic of research for the safe design of embedded retaining structures in seismic zones. Since the 1920s, pioneered by Okabe (1926) and Mononobe (1929), many researchers investigated seismic earth pressure on retaining structures with broadening interests and developed several methods with various assumptions/simplifications within the framework of static or equivalent static analysis to solve this complex problem. Even though these methods are still commonly used in engineering practice to determine dynamic soil pressures to account for seismic accelerations propagating in both horizontal and vertical directions, the importance of rigorous numerical analyses considering SSI effects is gradually being recognized and accepted by the researchers and engineers. This is not only due to concerns that the structural dynamic response changes with the combined soil-structural system under an applied earthquake, but also because the simplified static analysis may not always produce conservative results.

This section provides a critical literature review on the availability of analytical technologies and methodologies used to determine seismic-induced soil pressures on

embedded structures and their applicability in both the conventional and nuclear engineering fields. Limitations of the various methods and the potential issues to be further investigated are also identified and discussed.

3.2   EQUIVALENT STATIC ANALYSIS

Traditionally, neglecting SSI effects is believed to be conservative for the determination of seismic earth pressure, considering that the structure is becoming flexible when responding together with the soil. The seismic response is reduced with increased natural period and effective system damping. Neglecting the SSI tremendously simplifies the analysis, and gives a reasonable approximation to the maximum dynamic response of the structure to earthquake excitation. A well-developed static analysis method, representing the complex seismic dynamic effects by a simplified approach, is relatively simple and readily implemented in engineering projects, and is welcomed and accepted in the engineering practice.

The equivalent static analysis methods used for calculating dynamic soil pressures were developed mainly suitable for two types of wall systems, including: 1) yielding wall, which requires sufficient deformation to develop minimum active earth pressures; and 2) rigid wall, which is able to satisfy the required movement condition.

3.2.1 Yielding Wall Theory

Effects of ground motion on retaining walls were initially recognized by Okabe (1924) and Mononobe (1929) following the great Kanto earthquake of 1923. The M-O method was developed for dry, cohesionless soils following Coulomb's theory of static soil pressure and limit-equilibrium approach. It is a pseudo-static method based on the assumption that the retaining wall may yield under seismic impacts and produce sufficient movement to develop active earth pressure in soil behind the wall. As such, a soil wedge is formed with the shear strength being fully mobilized along the sliding surface at the limit state (see Figure 3-1).

Figure 3-1: Active Earth Pressure by the M-O method

The amount of wall movement required to develop active earth pressure is relatively small. A displacement of about 0.002H (H = the wall height) is enough to develop the active stress state. The triangle soil wedge is treated as a rigid body, with the vertical and horizontal inertial forces, $k_v W$ and $k_h W$ respectively, acting in conjunction with the weight of the soil wedge, as shown in Figure 3-1. Correspondingly, the vertical and horizontal seismic coefficients, k_v and k_h, can be determined by the vertical and horizontal ground accelerations divided by gravitational acceleration, respectively.

As illustrated in Figure 3-1, the total active soil pressure P_a during a seismic event includes a static component P_A and a dynamic one ΔP_{AE}, and can be determined as

$$P_a = P_A + \Delta P_{AE} = \frac{1}{2}\gamma H^2 (1 - k_v) K_{AE} \qquad \text{Eq. (2)}$$

in which, γ is the unit weight of the backfill soil, H is the height of the wall, and K_{AE} is the coefficient of active earth pressure, which is determined from

$$K_{AE} = \frac{\cos^2(\phi - \psi - \theta)}{\cos\theta \cdot \cos^2\psi \cdot \cos(\delta + \psi + \theta)\left[1 + \sqrt{\dfrac{\sin(\phi + \delta) \cdot \sin(\phi - \beta - \theta)}{\cos(\delta + \psi + \theta) \cdot \cos(\psi - \beta)}}\right]^2} \qquad \text{Eq. (3)}$$

where ϕ is the internal soil friction angle, δ is the frictional angle at the interface of the wall and backfill, ψ is the inclination angle at the contact surface of the structure, β is the slope inclination of the ground surface behind the wall, θ denotes seismic inertial angle relative to the gravity direction, and can be determined as

$$\theta = \tan^{-1}\left(\frac{k_h}{1-k_v}\right) \qquad\qquad \text{Eq. (4)}$$

When the earthquake induces sufficient wall movement towards backfill soil, the seismic-induced passive soil pressures P_p can be determined using Equation 2 by replacing K_{AE} with the coefficient of passive earth pressure K_{PE} expressed as

$$K_{PE} = \frac{\cos^2(\phi+\psi-\theta)}{\cos\theta\cdot\cos^2\psi\cdot\cos(\delta-\psi+\theta)\left[1-\sqrt{\dfrac{\sin(\phi+\delta)\cdot\sin(\phi+\beta-\theta)}{\cos(\delta-\psi+\theta)\cdot\cos(\psi-\beta)}}\right]^2} \qquad \text{Eq. (5)}$$

For the embedded perimeter walls of a structure, the angles ψ and β are generally zero. Consequently, Equations 3 and 5 can be further simplified as

$$K_{AE,PE} = \frac{\cos^2(\phi-\theta)}{\cos\theta\cdot\cos(\delta+\theta)\left[1\pm\sqrt{\dfrac{\sin(\phi+\delta)\cdot\sin(\phi-\theta)}{\cos(\delta+\theta)}}\right]^2} \qquad \text{Eq. (6)}$$

The length of the yielded soil wedge (see Figure 3-1) can be determined according to the inclination angle for the sliding plane as

$$L = H\cdot\cot\alpha = H\cdot\left[-\tan(\phi+\delta)+\sec(\phi+\delta)\sqrt{\frac{\cos(\phi+\delta+\theta)\cdot\sin(\phi+\delta)}{\sin(\phi-\theta)}}\right] \qquad \text{Eq. (7)}$$

It should be noted that Equation 6 is applicable only when the seismic initial angle θ is less than or equal to the internal soil friction angle ϕ. Beyond this limit, $K_{AE,PE}$ becomes unlimited and cannot be evaluated using the M-O method properly.

The variation of seismic soil pressure along the height of the wall was initially represented by an inverted triangle distribution with the maximum pressure at the ground surface. The application point of the dynamic thrust was initially taken acting at the elevation of H/3 from the base of the wall. However, later experimental results showed that the working point location ranges from H/2 to 2H/3 of the wall. Currently, 2H/3 is recommended in most codes and standards to avoid underestimating the overturning effects.

Comparisons between results from the M-O method and shaking table tests were reported in the literature (Ohara et al. [1970], Ishihara et al. [1973], Sherif et al. [1982], Ishibashi and Fang [1987]). For example, the test results by Ishibashi and Fang [1987] showed that, when the wall rotates about its bottom, the measured lateral pressure was approximately 23% to 43% higher than M-O theoretical results. For translation of the wall, the experimental values of lateral soil pressure were about 30% higher than those obtained from Equation 2 (Sherif et al. [1982]). However, it has been noted that the seismic loadings in these tests were limited to relatively low levels, and the amplitude of input acceleration was usually less than 500 cm/sec^2. In engineering practice, it is difficult to provide realistic results with the M-O approach when the design involves high ground accelerations and complex backfill conditions. In general, even though its limitations are

obvious, there has been a wide consensus in engineering practice that the M-O method is simple to use and can reasonably estimate the total seismic (dynamic) lateral soil pressure increment for retaining structures.

Owing to the limitation of the M-O method, considerable research has been carried out to find improved methods to evaluate seismic-induced earth pressure; see, for example, Seed and Whitman [1970], Richard and Elms [1979], Choudhury and Nimbalkar [2005], Koseki et al. [2007], among others. Based on a parametric sensitivity analysis, Seed and Whitman [1970] reformulated the seismic coefficient used in the M-O method and further proposed a solution suitable for practical application. The modified seismic soil pressure ΔP_{AE} is determined as

$$\Delta P_{AE} \approx \frac{3}{8} k_h \gamma H^2 \qquad \text{Eq. (8)}$$

The above equation is an approximate solution and represents a vertical wall with flat top backfill soil having the friction angle of approximately 35° quite well. The horizontal seismic coefficient k_h is recommended to choose the peak ground acceleration for the design seismic ground motions, and the resultant dynamic thrust acts at $0.6H$ above the bottom of the wall (i.e., inverted trapezoidal pressure distribution). This approximation has good agreement with results from dynamic FEM when $k_h \leq 0.35$ and $k_v = 0$.

Koseki et al. [2007] proposed another approach to modify the M-O method. In this approach, the effects of soil strain localization that develops on the failure plane are

taken into account. More specifically, the friction angle is assumed to decrease gradually

from the peak value ϕ_{peak} to the residual value ϕ_{res} with the increase of soil displacement.

As such, new active failure planes are mobilized during seismic loading with the variation

of soil state and the corresponding friction angle, as illustrated in Figure 3-2.
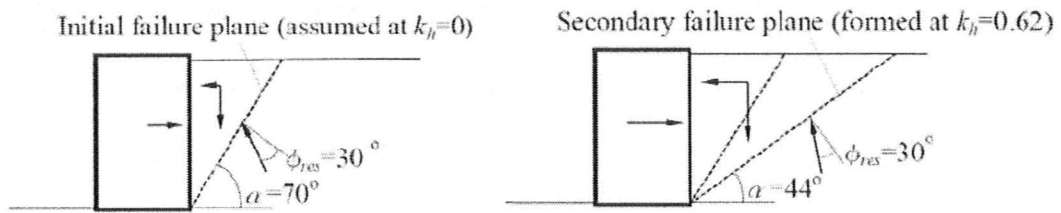
Figure 3-2: Initial and Secondary Active Failure Planes

When applying the method proposed by Koseki et al. [2007], both the peak and

residual shear resistances must be known and properly evaluated to reflect the compaction

level of backfill soil. After obtaining the initial failure plane under the ϕ_{peak} condition by

using the M-O method, the transformed coefficient of active earth pressure can be

calculated as

$$K'_{AE} = \frac{\cos(\alpha-\phi)\cdot(1+\tan\alpha)\cdot[\tan(\alpha-\phi)+\tan\theta]}{\tan\alpha\cdot\cos(\alpha-\phi-\delta)} \qquad \text{Eq. (9)}$$

in which, the reduced soil friction angle ϕ_{res} is used. Comparing the coefficient

determined by the M-O method using the value of ϕ_{peak}, the secondary failure plane may

develop in soil if K'_{AE} has a smaller value. In the proposed approach, evaluation based on the new failure plane is continued until a stable state is found. Since the post-peak reduction of the shear resistance in the backfill soil is considered, it is expected that this method produces more realistic results. In addition, this method can effectively overcome the limitation of the M-O method and can be adapted to analyses with a large horizontal seismic coefficient k_h when the initial seismic angle θ is larger than the internal soil friction angle ϕ. Currently, Koseki's approach is recommended by the Architectural Institute of Japan (AIJ) for the determination of seismic soil pressures on retaining structures.

Comparable with the above discussed force-based analysis methods, the displacement-based analysis method initially proposed by Newmark [1965] assumes that the retaining structure moves with the backfill soil under an earthquake. The permissible displacement under seismic conditions is determined by considering the relative motion of a rigid block when the ground acceleration exceeds the yield acceleration of the block. The resistance to the motion is governed by the shearing resistance between the block and the ground. Based on allowable permanent wall displacements, Richard and Elms [1979] introduced a method for the seismic design of yielding walls by considering translational sliding as the failure mode. However, this method is not suitable for deeply embedded structures, since the movement of the wall requires relative large movements that may not be achieved. So far, only Eurocode 8 adopts this kind of performance-based approach to determine the horizontal acceleration coefficient k_h, and then works it together with the M-O method for the design of retaining structures.

Currently, there is an opinion in the nuclear engineering industry that the seismic-induced passive earth pressure should be used as a sole criterion to produce a conservative design for safety related structures. When the relative foundation displacement is sufficient to result in passive state in soil, the seismic passive soil pressure is generally approximately 10 times greater than the corresponding active pressure. As such, maximum pressure distribution on the wall is controlled by the passive earth pressure rather than the active soil pressure obtained from the M-O method. However, appropriate and reasonable criteria and coefficients must be applied, based on further investigation and verification when designating the passive earth pressure to design deeply embedded structures.

3.2.2 Rigid Wall Theory

Recall that the Mononobe-Okabe theory was developed for the design of retaining walls that have relatively large displacements during an earthquake to develop a sliding soil wedge or the active state. For the basement walls of a structure, relatively large movement between the wall and soil is impossible to develop and hence the conditions assumed in the Mononobe-Okabe theory cannot be satisfied. A basement wall can be considered as a rigid, non-yielding wall (Wood [1973]), which is different from the yield wall assumed in the Mononobe-Okabe theory. This concern has been confirmed by field observations and experimental data, along with enhanced analytical methods and techniques. With better understanding on the interaction between the soil and structure, it has been noted that the dynamic behavior between the yield wall and rigid wall have significant differences. The seismic-induced soil pressure is a function of all combined

parameters that affect soil-structure interaction responses. The erroneous application of M-O method underestimates the active pressures and overestimates the passive pressures when analyzing a relatively rigid structure with deep embedment.
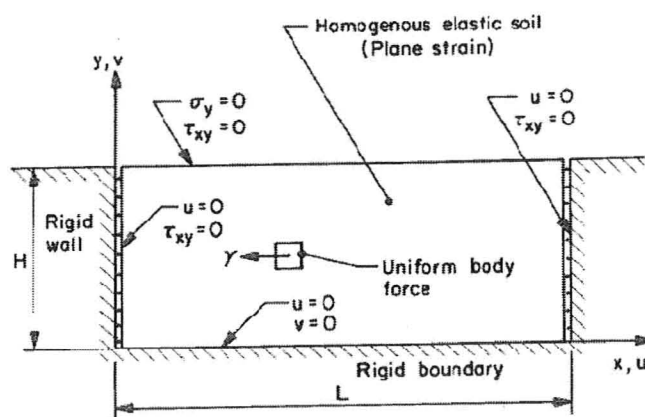
Figure 3-3: Rigid Wall Model by Wood [1973]

Wood [1973] developed an equivalent static solution for dynamic soil pressure on rigid (non-yielding) walls by using the linear elastic FE method. In his model (as shown in Figure 3-3), rigid walls retain a homogeneous linearly elastic soil with finite length. Smooth contact between the wall and soil is assumed to neglect the shear stresses along the vertical boundaries. Both the wall and soil are anchored to a rigid base. The harmonic base excitation is represented by a one "g" horizontal acceleration. A uniform horizontal body force is assumed to act throughout the soil layer, and hence the nonlinear behavior

34

of soil can be neglected. The seismic-induced soil pressure distribution is simply determined by the earthquake-generated body forces in the soil.

Under the plane strain condition, the equilibrium equations for a homogeneous, linear elastic, isotropic medium are

$$\frac{\partial \sigma_x}{\partial x} + \frac{\partial \tau_{xy}}{\partial y} + F_x = 0$$

$$\frac{\partial \sigma_y}{\partial y} + \frac{\partial \tau_{xy}}{\partial x} + F_y = 0$$

Eq. (10)

in which, σ_x, σ_y = normal stresses in the x and y directions, respectively; τ_{xy} = shear stress in the soil; F_x, F_y = the components of body forces per unit volume in the x and y directions, respectively. In addition, the stress-strain relations are expressed as

$$\frac{\sigma_x}{G} = k^2 \frac{\partial u}{\partial x} + (k^2 - 2)\frac{\partial v}{\partial y}$$

$$\frac{\sigma_y}{G} = (k^2 - 2)\frac{\partial u}{\partial x} + k^2 \frac{\partial v}{\partial y}$$

Eq. (11)

$$\frac{\tau_{xy}}{G} = \frac{\partial u}{\partial y} + \frac{\partial v}{\partial x}$$

in which, $k^2 = \left(\frac{V_d}{V_s}\right)^2 = \frac{2(1-v)}{1-2\cdot v}$, with G = shear modulus of the soil, V_d = dilatational wave speed, V_s = shear wave speed, v = Poisson's ratio of the soil. The equilibrium equations are further expressed in terms of the displacements after substituting Equation 11 into Equation 10 as follows:

$$k^2 \frac{\partial^2 u}{\partial x^2} + (k^2 - 1)\frac{\partial^2 v}{\partial x \cdot \partial y} + \frac{\partial^2 u}{\partial y^2} = \frac{\gamma}{G}$$

$$k^2 \frac{\partial^2 v}{\partial x^2} + (k^2 - 1)\frac{\partial^2 u}{\partial x \cdot \partial y} + \frac{\partial^2 v}{\partial x^2} = 0$$

Eq. (12)

After applying the boundary conditions and performing mathematical operations, the dimensionless seismic soil lateral pressures applied onto the smooth rigid wall can be simplified and conservatively determined, as summarized in Figure 3-4. The resultant thrust force associated with dynamic stress distribution shown in Figure 3-4 can be determined as

$$\Delta P_E = C_v k_h \gamma H^2$$

Eq. (13)
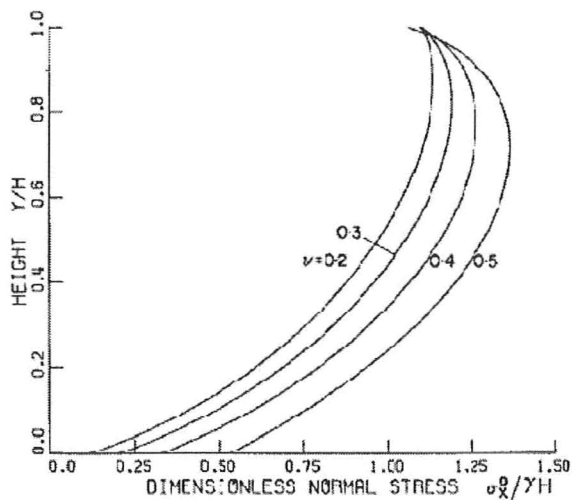
Figure 3-4: Soil Lateral Pressure Distribution (Wood [1973])

36

in which, k_h is the maximum horizontal earthquake acceleration, C_v is the force coefficient as a function of Poisson's ratio of the soil medium. Figure 3-5 presents the variation of the dimensionless seismic soil pressure with L/H ratio with H being the wall height and L the horizontal distance between the walls (as shown in Figure 3-3). It is recommended that the resultant dynamic thrust force is located at the point of 0.6 of the total embedment depth measuring from the wall's base.
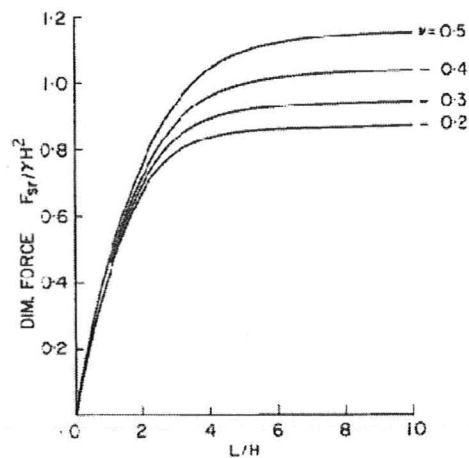
Figure 3-5: Lateral Force Coefficient (Wood [1973])

Wood [1973] also provided an approximate analytical solution that gave good estimates of the peak seismic thrust for harmonic base excitation when dynamic amplification effects in the wall-soil system were negligible. He noticed that the dynamic amplification is insignificant for relatively low-frequency ground motions, and it could be

neglected when the frequency ratio (f_0/f_s) is less than about 0.5. Herein f_0 is the frequency of harmonic motion, and f_s represents the cyclic frequency of the backfill soil's first shear mode. f_s can be determined as $f_s = V_s/4H$ with H being the embedment depth and V_s the shear wave velocity of soil.

The standard ASCE 4-98 recommends Wood's pressure diagram (based on one "g" static loading of the soil-structural system) as an effective and reasonable solution to estimate dynamic pressure on embedded perimeter retaining walls for nuclear structures when no significant structure-structure interaction is anticipated. However, the solution proposed by Wood does not consider the effects due to the inertial response of the superstructures. These effects may change the response of overall soil-structural system significantly, which affect the lateral dynamic soil pressures that should be superposed from the superstructure displacement and the seismic generated soil body forces. Following Wood's work, Veletsos et al. [1994] performed more detailed analysis by incorporating the effects of wave propagation and seismic motion amplification. However, their solution is mathematically complicated for engineering applications.

Ostadan [2005] investigated the characteristics of lateral seismic soil pressures based on a series of seismic SSI analyses using computer program SASSI 2000, and developed a simple method for building walls rather than retaining walls. His method took into account most main parameters affecting seismic soil pressure, including soil nonlinearity, wave propagation in the soil media, the site's specific dynamic soil properties, and design motion characteristics. According to Ostadan [2005], the dynamic characteristics of earth pressure amplitudes are similar to a single-degree-of-freedom

(SDOF) system with respect to the ground motion's frequency, and the system's dynamic response is controlled by the stiffness at long period, the damping at resonance and the inertia at short period. He found that the maximum amplification of the pressure response is controlled by radiation damping due to the soil's continuity behind the wall, and occurs at the harmonic frequency corresponding to the soil column's natural frequency f_s.

The computational steps recommended by Ostadan [2005] to determine the lateral seismic soil pressure for deeply embedded structures are as follows:

1. Perform an analysis for a free-field soil column and obtain the response motion of the ground in terms of acceleration response spectrum at the depth corresponding to the base of the wall in the free-field. The response motion should be obtained at 30 percent damping considering high levels of radiation damping. The analysis of free-field soil columns can be performed using an available computer program with input motion specified either at the ground surface or at the depth of the foundation base. The choice for the location of control motion should be consistent with the development of design motion.

2. Utilize equations proposed by Veletsos et al. [1994] to determine the total soil mass (m) for a representative SDOF system using Poisson's ratio (v) and density of the soil:

$$m = 0.5\rho H^2 \Psi_v \qquad\qquad \text{Eq. (14)}$$

in which, ρ is the density of the soil, H is the embedment height of the wall, and Ψ_ν is a factor adjustable for different values of the soil's Poisson's ratio expressed as

$$\Psi_\nu = \frac{2}{\sqrt{(1-\nu)(2-\nu)}}$$ Eq. (15)

3. Calculate the total lateral seismic force F_{Total} by multiplying the total soil mass determined in step 2 with the acceleration spectral amplitude (S_a) of the free-field response at the soil column frequency obtained from step 1:

$$F_{Total} = m \cdot S_a$$ Eq. (16)

The corresponding soil column frequency (f_s) can be determined by computer program or the following simplified relation

$$f_s = V_s / 4H$$ Eq. (17)

where V_s represents the average strain-compatible shear wave velocity of the soil column over the embedment of the wall.

4. Determine the maximum lateral seismic soil pressure at the ground surface level by dividing the total lateral seismic force as obtained in Step 3 by the area ($= 0.744H$) associated with the normalized seismic soil pressure curve.

5. Obtain the normalized pressure distribution by multiplying the above maximum lateral earth pressure with the pressure distribution function given as

$$p_y = -0.0015 + 5.05y - 15.84y^2 + 28.25y^3 - 24.59y^4 + 8.14y^5 \qquad \text{Eq. (18)}$$

in which, the normalized height ratio ($y = Y/H$) ranges between zero at the bottom of the wall and one at the top of the wall, and Y equals the distance measured from the base of the wall.

In addition to verifying the accuracy of the simplified method using direct dynamic FE analyses, Ostadan [2005] provided a comparison of his method with commonly used methods including both the M-O method and that proposed by Wood [1973]. He concluded that this method has a lower limit according to the M-O method but an upper limit by the Wood solution. The proposed method generates a wide range of pressure profiles, depending on the dynamic properties of the backfill soil, as well as the frequency characteristics of the input ground motion. In general, Ostadan's method is adequate to estimate a conservative maximum seismic soil pressure for a rigid wall on a rigid base boundary, even though it is limited by only incorporating the kinematic interaction effects without properly addressing the inertia effects of the superstructure on determining seismic-induced soil pressure. Currently, this method has been adopted by the NEHRP standard (i.e., FEMA 750-2009) and is being proposed to be incorporated in the new release of ASCE 4 standard.

Owing to the frequent earthquake occurrences in Japan, typical BWR containment buildings are intentionally designed with deep embedment. Research has been performed focusing on the fundamental characteristics of seismic-induced soil pressures to develop the methodologies to quantify the seismic pressure on the embedment. Nukui et al. [1989]

proposed a simplified method to estimate the dynamic soil pressure distribution for deeply embedded rigid structures. Currently, this method is widely used in Japanese nuclear industry.
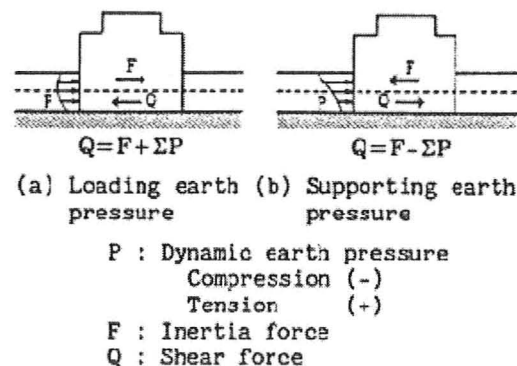
Figure 3-6: Loading and Supporting Earth Pressures (Nukui [1989])

Nukui et al. [1989] considered the inertial force induced by the superstructure and classified the dynamic soil pressures as two types, as illustrated in Figure 3-6. One is called the loading (active) earth pressure acting in the same direction as the inertial force of the building, and the other is termed as supporting (passive) earth pressure, which is applied in the opposite direction against the inertial force. The resultant dynamic earth pressure (P) at the loading side is approximately determined by utilizing Tajimi's equation (Tajimi, [1985]).

$$P = \frac{\sqrt{3(1+v)}}{4} \rho H^2 A \qquad\qquad\text{Eq. (19)}$$

in which, v, ρ, H have standard definitions as described previously, A represents the ground acceleration. If the maximum acceleration (A_{max}) at the ground surface is used and the earth pressure distribution is assumed to be uniform along embedded depth, the above equation is bounded to $P_a = 0.6\rho H A_{max}$.

The resultant lateral pressure (P_s) at the supporting side is determined according to the total inertial force (F) of the structure and the shear ratio (β) of the surrounding soil as

$$P_S = \beta F \qquad\qquad\text{Eq. (20)}$$

where the total inertial force (F) is calculated based on the maximum acceleration distribution of the structure, which should be reduced for the embedded section when the maximum supporting earth pressure occurs. The shear ratio of the surrounding soil (β) should be evaluated from the reaction forces when applying static unit loading to the structure, and can be conservatively simplified as

$$\beta = \frac{K}{2(1+K)} \qquad\qquad\text{Eq. (21)}$$

$$K = \frac{(H/L)}{0.06 + 0.15(H/L)}\left(\frac{V_{SE}}{V_{SD}}\right)^2 \qquad\qquad\text{Eq. (22)}$$

in which, H is the thickness of the surface soil layer, L represents the building width or diameter, V_{SE} is the mean shear wave velocity of the surrounding soil, and V_{SD} is the

shear wave velocity of the bedrock. In addition, the earth pressure on the supporting side is assumed to be static and linearly distributed. The maximum pressure at the ground surface is $1.5P_s$, while the minimum pressure at the base of embedment equals $0.5P_s$. The applicability of this simplified method was verified by comparisons with the results of detailed dynamic FEM analyses. It was found that the dynamic earth pressures dominantly act on either the loading side or the supporting side, depending on whether the surface soil layer is soft or hard. From the study, it was confirmed that the simple solutions proposed by Nukui et al. [1989] would be applicable to evaluate the dynamic earth pressure for the design of a NPP reactor building.

3.3   DYNAMIC ANALYSIS

The seismic analysis for deeply embedded structures requires a comprehensive knowledge of earth pressures under both active and passive conditions. The conventional, simplified methods discussed in the previous section are deemed to be conservative when used in engineering practice. However, these methods are established on assumptions, which may not be always truly achievable, hence they may only be valid for certain class of structures and soil conditions. In addition, these simplified methods neglect the effects of some important factors, which may include the nonlinearity of backfill soil, the contact behavior at the interface of the soil and structure, the time-dependent effects of applied earthquake ground motion, the effect of variation in soil parameters (e.g., internal friction angle, damping ratio and Poisson's ratio, shear moduli, etc.) under seismic

loading, the effect of seismic shear and primary wave velocities in the backfill soil, hydrodynamic effects of pore water, etc.

From rigorous numerical analyses considering the SSI effects, some researchers noticed that a structure with long natural period is not always beneficial to the overall system as assumed by the simplified design, since resonance may take place at long period ground motions associated with soft soil media. Correspondingly, the ductility effects become more significant with the increase of the structural response period. Any permanent deformation and failure of soil will further deteriorate the seismic response of the structure and increase the lateral earth pressures. In fact, the structural dynamic response must be properly addressed by considering the SSI effects in the overall structural system. Neglecting the SSI effects in an analysis may lead to unsafe design for the safety related structures of a nuclear power plant (NPP). Fortunately, with the fast development of computer technology, modeling the overall soil-structure system incorporating the dynamic effects is becoming easier.

3.3.1 Pseudo-Dynamic Analysis

As discussed in the previous section, it is not realistic to utilize the equivalent static analysis methods to determine the complex response of retaining structures under seismic condition. To overcome the shortcoming, several pseudo-dynamic methods have been developed recently by incorporating time-dependent dynamic effects and the variation of system parameters by means of certain simplifications (e.g., Steedman and Zeng [1990], Wu and Finn [1999], Choudhury and Nimbalkar [2005]). The phase

difference due to the propagation of shear wave and the amplification effect within the soil media are addressed together with the ground accelerations. It has been found that the pseudo-dynamic method is capable of providing more reasonable solutions for the distribution of dynamic earth pressures induced by seismic motion.

Wu and Finn [1999] utilized an analytical approximation to determine the seismic response of a soil-retaining wall system and the seismic earth pressure. In order to make the solution simple, only relative horizontal displacement between the backfill and the rigid base was taken into consideration. The equation of motion for the backfill soil under a base acceleration $\ddot{u}_b(t)$ in the horizontal (or the x – direction) is expressed as

$$G\frac{\partial^2 u}{\partial y^2}+\frac{2}{1-v}G\frac{\partial^2 u}{\partial x^2}-\rho\frac{\partial^2 u}{\partial t^2}=\rho\ddot{u}_b(t)$$

Eq. (23)

The corresponding normal stress in the x-direction is determined as

$$\sigma_x=\frac{2}{1-v}G\frac{\partial u}{\partial x}$$

Eq. (24)

The total dynamic thrust force applied to the rigid wall can be determined by integration of distributed lateral dynamic soil pressure over the height of the wall:

$$Q(t)=\int_0^H p(t)dy=\frac{2G}{1-v}\sum_{m=1}^{\infty}\sum_{n=1}^{\infty}\frac{16f_{mn}(t)}{\pi^2(2n-1)^2(L/H)}$$

Eq. (25)

with H being the wall height and L the horizontal distance between two boundaries (see Figure 3-3). The transient modal solution $f_{mn}(t)$ is determined by solving the following equation:

$$\ddot{f}_{mn}(t) + 2\lambda\omega_{mn}\dot{f}_{mn}(t) + \omega_{mn}^2 f_{mn}(t) = -\ddot{u}_b(t)$$

Eq. (26)

When subjecting to a harmonic base excitation $\ddot{u}_b(t) = A_{max}e^{i\omega t}$, the steady-state response $f_{mn}(t)$ is calculated as

$$f_{mn}(t) = -\frac{A_{max}e^{i\omega t}}{\left(\omega_{mn}^2 - \omega^2\right) + 2i\lambda\omega_{mn}\omega}$$

Eq. (27)

The fundamental frequency (ω_{11}) of wall-soil systems can be computed directly by performing dynamic analysis. However, to facilitate the use of design charts in practice, the fundamental frequency can be approximated as

$$\omega_{11} = \frac{\pi}{2H}\sqrt{\frac{G}{\rho}\left(1 + \frac{2}{1-v}\frac{H^2}{L^2}\right)}$$

Eq. (28)

Wu and Finn [1999] modified the conventional shear beam models based on studies performed by Wood [1973] and Veletsos et al. [1994], and developed a family of design charts for seismic-induced pressures against rigid walls to simplify the complicated analysis process. The effect of variation in soil properties with depth (or vertical stress level) is accounted for by making the shear modulus of soil varying with depth as one of the three forms: uniform distribution, linear-triangle and parabolic variations. These design charts envelop large numbers of combinations of ground acceleration and the distribution of shear modulus of backfill soil along the depth. In the charts shown in Figure 3-7, the normalized thrusts ratios $Q/\left(\rho H^2 A_{max}\right)$ are expressed as

functions of frequency ratios ω/ω_{11} with ω representing the base acceleration frequency of the earthquake motion.

Wu and Finn verified their approximate solutions using nonlinear FE dynamic analysis and compared the results with other equivalent static solutions (e.g. Wood [1973] and the M-O method). They concluded that Wood's static solution is suitable for estimating the peak dynamic thrusts under harmonic excitation for a low frequency ratio ($\omega/\omega_{11} < 0.2$), but the seismic thrusts tend to be overestimated for frequency ratio $\omega/\omega_{11} > 2$. When the soil-wall system is approaching resonance at $\omega/\omega_{11} \approx 1$, Wood's static solution may significantly underestimate the magnitude of dynamic lateral forces (up to about 40 percent or higher).

Wu and Finn also studied the effects on seismic pressures by the variations of damping ratios λ and Poisson's ratios μ of the backfill soil (See Figure 3-7 for details). For different types of backfill soils, the location of the resultant seismic force on the wall was found to vary between 0.5H to 0.64H from the bottom. Moreover, they noticed that the nonlinear soil behavior resulted in increasing the total seismic force against the rigid wall due to reduced modulus and increased damping of the system.
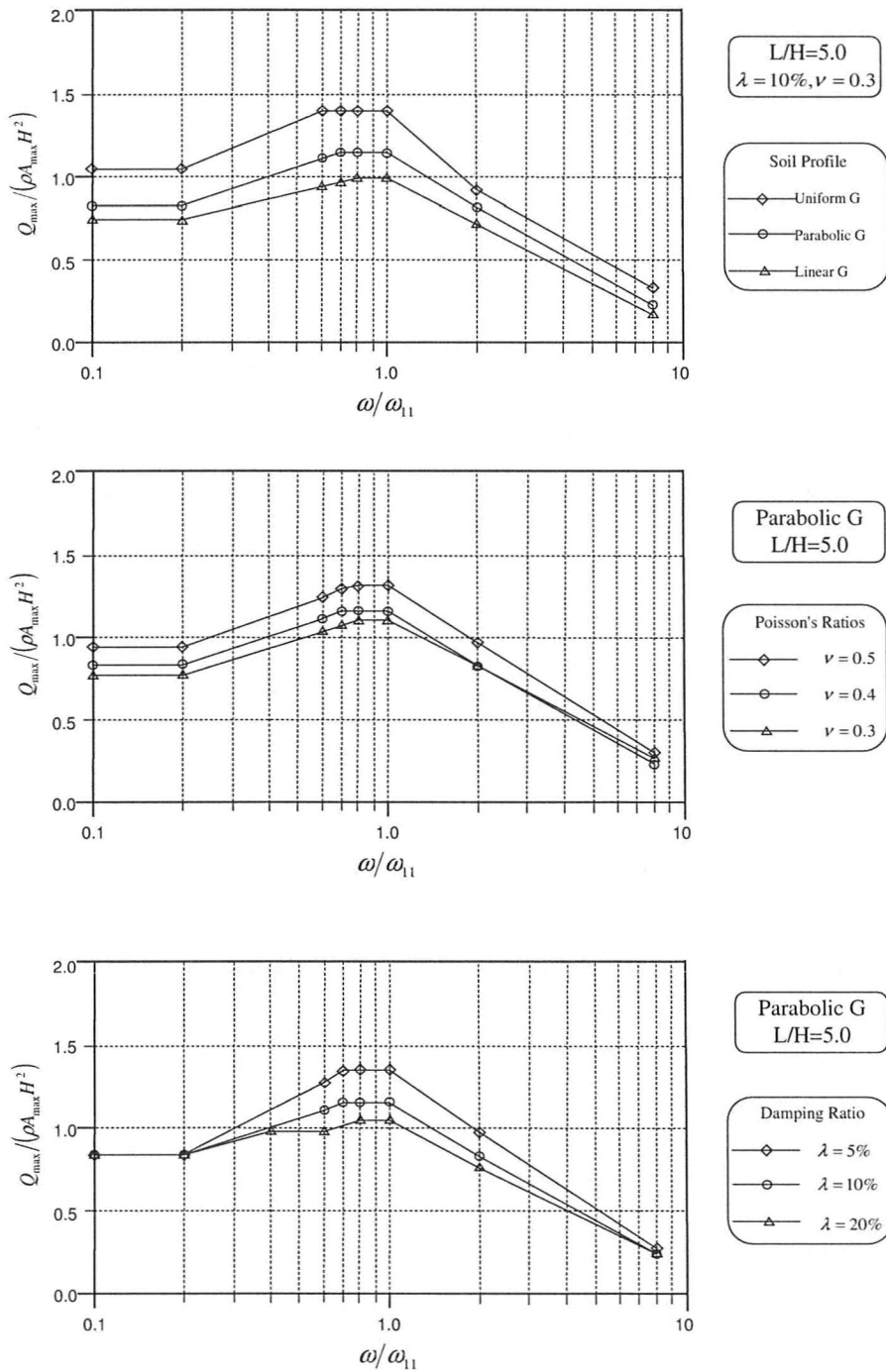
Figure 3-7: Design Charts for Peak Seismic Thrusts (Wu [1999])

By improving the idea initially proposed by Steedman and Zeng [1990], Choudhury and Nimbalkar [2005] developed a pseudo-dynamic approach to determine the seismic resistance of an embedded structure against both active and passive earth pressures. This approach considers both horizontal and vertical seismic accelerations as well as the variable seismic parameters. More specifically, it deals with constant shear moduli of the backfill soil and assumes that the ground acceleration is variable in the phase rather than the magnitude. Similar to the M-O method, a rupture plane inclined at an angle (α) is assumed to simplify the analysis. The computation models for determining the dynamic soil pressures are illustrated in Figure 3-8.
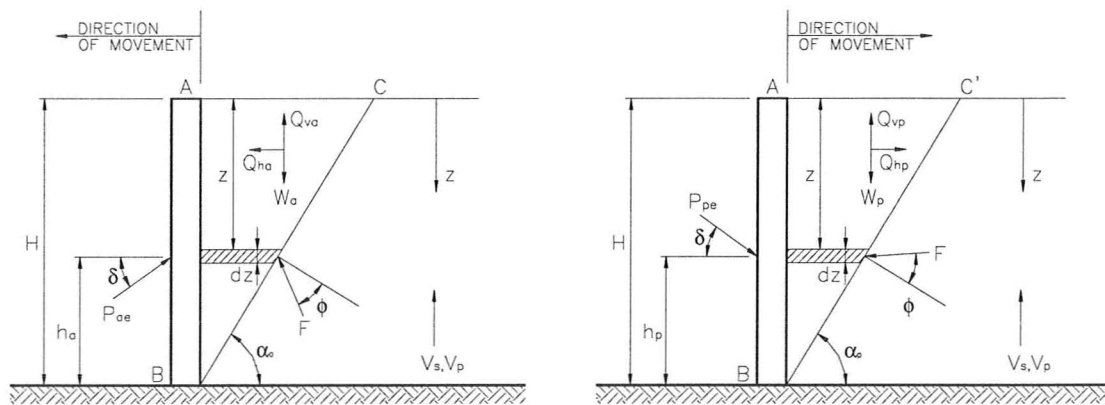
Figure 3-8: Computation Models for Determining Pseudo-Dynamic Soil Pressures

(Choudhury and Nimbalkar [2005])

When the base is subjecting to harmonic horizontal and vertical accelerations (a_h and a_v, respectively), the corresponding accelerations at any depth (z) and time (t) is expressed as

$$a_h(z,t) = a_h \sin \omega\left(t - \frac{H-z}{V_S}\right)$$

Eq. (29)

$$a_v(z,t) = a_v \sin \omega\left(t - \frac{H-z}{V_P}\right)$$

Eq. (30)

where H is wall height, V_S and V_P are the velocities of the shear wave and primary wave, respectively. The total horizontal and vertical inertia forces applied to the wall is determined via

$$\begin{aligned}
Q_h(t) &= \int_0^H m(z) \cdot a_h(z,t) \cdot dz \\
&= \frac{\lambda \gamma a_h}{4\pi^2 g \tan \alpha} \left[2\pi H \cos \omega\zeta + \lambda(\sin \omega\zeta - \sin \omega t)\right]
\end{aligned}$$

Eq. (31)

$$\begin{aligned}
Q_v(t) &= \int_0^H m(z) \cdot a_v(z,t) \cdot dz \\
&= \frac{\eta \gamma a_v}{4\pi^2 g \tan \alpha} \left[2\pi H \cos \omega\psi + \lambda(\sin \omega\psi - \sin \omega t)\right]
\end{aligned}$$

Eq. (32)

in which, α should be taken as α_a or α_p to calculate the active and passive earth pressures separately; $\lambda = TV_S$ and $\eta = TV_P$ present the wavelength of the vertically propagating shear wave and primary wave, respectively, with T being the corresponding wave period; $\zeta = t - H/V_S$ and $\psi = t - H/V_P$.

By differentiating the total (static and dynamic) thrust forces with respect to embedded depth z, the distribution of seismic active and passive earth pressures is obtained as follows:

$$
\begin{aligned}
p_{ae,pe} = & \frac{\gamma z}{\tan\alpha} \frac{\sin(\alpha\mp\varphi)}{\cos(\delta+\varphi\mp\alpha)} \pm \frac{k_h\gamma z}{\tan\alpha} \frac{\cos(\alpha\mp\varphi)}{\cos(\delta+\varphi\mp\alpha)} \sin\omega\left(t-\frac{z}{V_S}\right) \\
& \pm \frac{k_v\gamma z}{\tan\alpha} \frac{\sin(\alpha\mp\varphi)}{\cos(\delta+\varphi\mp\alpha)} \sin\omega\left(t-\frac{z}{V_P}\right)
\end{aligned}
$$

Eq. (33)

Compared to the equivalent static analysis (e.g. the M-O method), the pseudo-dynamic method proposed by Choudhury and Nimbalkar [2005] yields larger active pressures and smaller passive pressures with non-linear distributions along the height of wall under seismic conditions.

3.3.2 SSI Effects on Embedded Structures

The concept of soil structural interaction (SSI) under seismic conditions has been developed for decades and has received considerable attention in both research and engineering application. The determination of seismic-induced earth pressure on embedded structures as discussed in the previous sections is a special problem related to SSI. As demonstrated by the work of Wood [1973], Veletsos et al. [1994], and Ostadan [2005] among others, the determination of the dynamic lateral earth pressures is primarily governed by the SSI effects rather than the traditional concept of limiting equilibrium (i.e., the M-O method).

For structures (other than retaining walls) with embedded sections, the SSI is generally referred to the structural dynamic response when the structure is coupled with the surrounding soil medium. This coupled response is significantly different than that in the free field motion and depends on the characteristics of the seismic ground motion, the surrounding soil properties, as well as the structure itself. As illustrated in Figure 3-9, Tseng et al. [1991] summarizes the following five basic problems to be solved for the application of SSI analysis when subjecting to earthquake excitations:

1. Site response problem to determine the free field ground motions;

2. Foundation scattering problem to determine the modified seismic inputs due to the presence of the soil excavation and the boundary conditions at the soil-structure interface;

3. Structural modeling problem to determine the dynamic properties of the structure;

4. Foundation impedance problem to determine the dynamic force-displacement relations for the foundation medium;

5. Interaction response analysis problem to determine the dynamic response of the coupled soil-structure system.
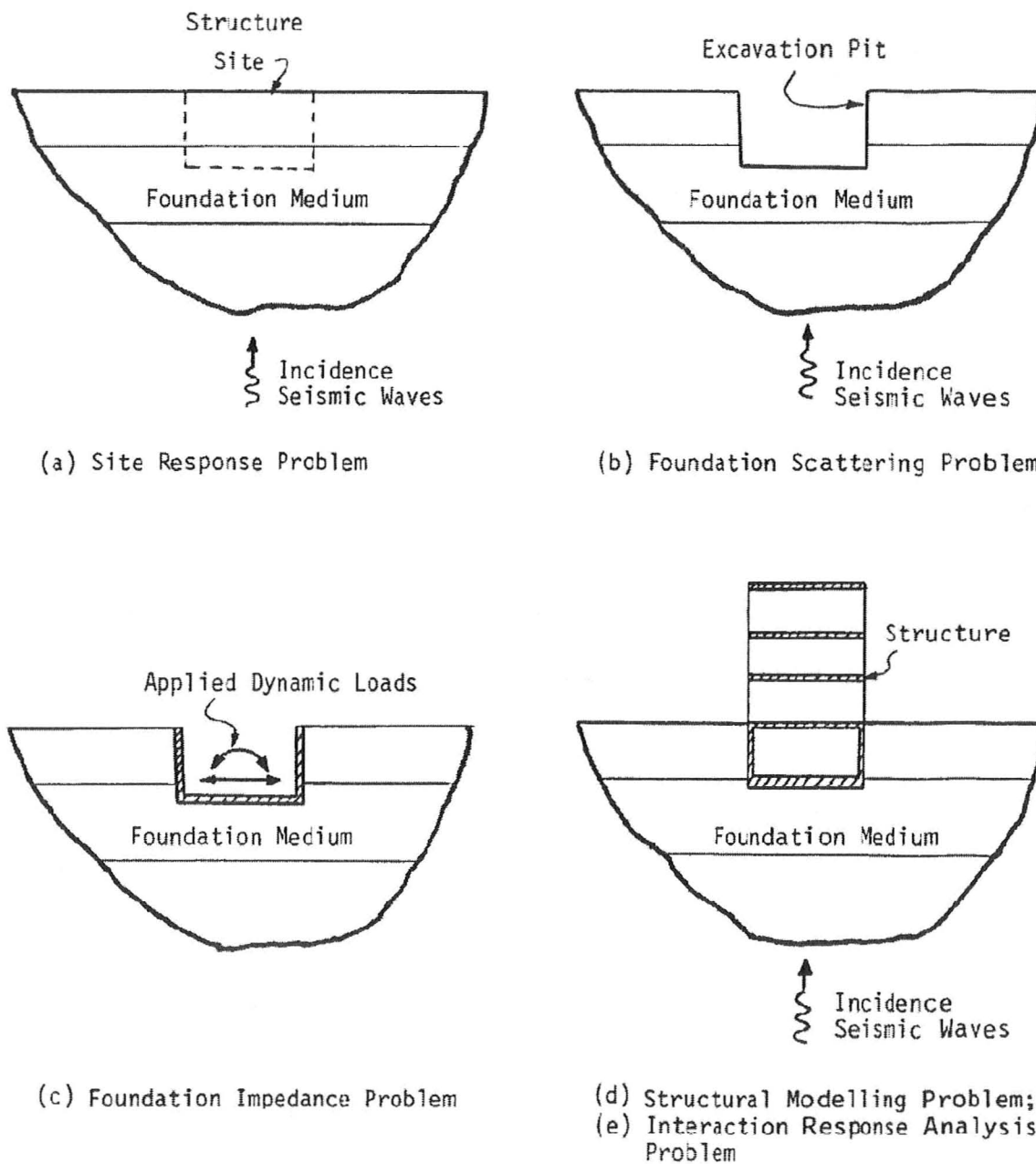
Figure 3-9: Illustration of the Basic Problems of Seismic SSI Analysis (Tseng, [1991])

In general, soil-structure interaction can be divided into two phenomena (Wolf, [1985]): a kinematic interaction, which represents the interaction of a massless rigid wall with the adjacent soil as modeled by Wood [1973], and an inertial interaction, which shows the interaction of the wall with the adjacent soil when connected to a responding superstructure. It has been recognized that the seismic soil pressure is affected not only by the kinematic interaction of the foundation, but also by the inertia effect of the superstructure. When subjected to an earthquake excitation, the incapability of the foundation to follow the response of free-field ground motion causes the kinematic interaction with the surrounding soil. In turn, the inertial force of superstructure is transferred further down to the soil, which causes more deformation in the soil due to the inertial interaction. Different than inertial interaction, the kinematic interaction effects are associated with the modification of the free-field motion due to the structural rigidity of the embedment and are therefore independent of the inertial properties of the structure. The inertial interaction, on the other hand, is associated with the dynamic response of the coupled structure-foundation system, which is mainly governed by the inertial properties of the structure and dynamic stiffness functions of the foundation.

When a structure is shallow embedded, its seismic response is primarily affected by the inertial interaction. With increasing embedment depth, the effect of the inertial interaction decreases and its counterpart, kinematic interaction, contributes more to the seismic response. If the structure is fully embedded underground, its seismic response is mainly controlled by the kinematic interaction effect and the inertial effect becomes minimal. Detailed SSI analyses incorporating both kinematic and inertial interactions

must be considered to determine seismic-induced earth pressures when performing the design for NPP safety related structures. According to Tseng [1991], the effects of SSI on the seismic response of structures with deep embedment may include the following issues:

1. The foundation impedance is intensified when increasing embedded depth, thus, causing an increase in the natural frequency of overall soil-structural system. The frequency change depends on the relative stiffness of the structure with respect to the soil.

2. The overall effective system damping increases. The main factor contributing to the increase in damping is the loss of energy by radiation of waves away from the foundation.

3. Both above-mentioned effects highly rely on the dynamic relative stiffness at the contact boundary, which increases with embedded depth, therefore, resulting in a decrease in the inertial interaction effect.

4. The rotational components at the foundation base are introduced when subjected to horizontal motion.

Depending on the characteristics of seismic input motions and the base frequency of the structure, the frequency increase resulting from SSI may not be helpful in reducing the seismic response; but an increase in the effective damping is always beneficial in amplitude reduction. Apparently, the kinematic effect is beneficial to the seismic response of deeply embedded structures. However, the effect is not clear as demonstrated by

experimental data. In addition, owing to the nature of the problem, the exact solution on the kinematic interaction effect is complicated and difficult to achieve by simplified approaches (Xu [2005]). Usually, numerical approaches (e.g., finite element method or boundary element method) utilizing a computer program must be used for the analysis of kinematic interaction effects.

The nonlinear behavior of the soil-structure system must also be properly addressed in the structural dynamic analysis with SSI. The primary nonlinearity in an analysis of SSI is associated with *the nonlinear behavior of soil media* under the seismic excitation alone without the involvement of structural response, while the secondary nonlinearity involves *the structural response* due to the effect of soil-structure interaction. Both nonlinearities have to be considered in the SSI analysis as required by codes and standards.

In general, the nonlinear behavior is caused by three reasons: geometric nonlinearity, material nonlinearity and boundary nonlinearity. Except for the geometric nonlinearity, which depends on the physical characteristics of the structure and may not be changed, it is found acceptable to simplify or approximate the material and boundary (or interface) nonlinearities by iterative linear elastic solutions. The boundary (or interface) nonlinearity exists in most soil-structure interaction problems when a deformable object comes in contact or separation with the other. The nature of this interface is an important aspect for the soil-structure interaction problem and has significant impact on the evaluation of seismic-induced soil pressures. One key objective

of this report is to investigate how the contact effects affect the overall system responses and the distribution of lateral seismic soil pressure along the embedment.

3.3.3 Numerical Methods for SSI Problems

In a broad sense, the analytical techniques used for numerical simulation for the seismic response of deeply embedded structures can be categorized by the following aspects:

1. Solving the problem by either the continuum or discrete approach;

2. Simulating the system using either a detailed or simplified model;

3. Utilizing either the direct solution or sub-structure (impedance) solution.

Depending on the characteristics of the physical problems to be analyzed, factors such as linear or non-linear material and geometric conditions may influence the choice of methods (either time domain or frequency domain techniques) for seismic analysis more, as compared to the size of models and computational efficiency.

The discrete approach applies the finite element method (FEM) to find approximate solutions of partial differential equations (PDE). while the continuum approach utilizes the boundary element method (BEM) by solving the boundary integral equations. Engineering practice often takes advantage of both approaches by modeling the near field with finite element method and the far field with boundary element method. The combined BEM-FEM approach is found more suitable for analyzing deeply embedded structures or uneven arranged backfills adjacent to embedded structures.

Romanel et al. [1993] utilized this method to study the seismic response of massive structures embedded in layered soils. In their model, the foundation and near field soils were discretized by finite elements and the BEM was employed to overcome difficulties associated with the boundary conditions that arise from modeling the infinite soil domain. The numerical solution for the SSI system is obtained by coupling the FEM with the BEM through compatibility and equilibrium conditions at the interfaces between soil-structure and different soil layer.

Usually, the continuum approach simulates the seismic wave propagation within a finite domain in a half-space. To avoid the effects of reflected waves or minimize their amplitude when reaching back to the structure, appropriate dampers (dashpots) are applied at the far side boundaries of the finite soil domain to absorb the redundant wave energy. As an alternative, the boundary limits have to be arranged further away from the central area to mitigate wave reflection within acceptable intensity. In order to represent major characteristics of soil-structural system, the finite element type selection needs to consider the theory, which the element is based on. When defining the discretization parameters, various aspects such as the element size, shape, and aspect ratio, the internal node points and the number of nodes representing each element should be considered.

A detailed or simplified approach is defined to differentiate the applications between the FEM-BEM models or lumped mass parameter models, respectively (Xu [2005]). The detailed approach is more suitable and reliable to capture the various effects of a combined soil-structure system, but it requires significant computational efforts. On the other hand, the simplified method (or the lumped parameter method) is generally

implemented using constant stiffness and damping coefficients as transmitting boundaries to simplify the SSI effects, therefore, it is easy for implementation but may not be able to properly characterize or predict the distribution of seismic-induced soil pressure. The stiffness and damping coefficients in the lumped parameter method are generally termed as SSI coefficients that represent the dynamic characteristics of the soil-structure system. They can be determined using conventional analytic solutions assuming a rigid foundation on a half-space consisting of uniform or layered soils. Depending on the particular formulation to be applied, the dynamic stiffness can be either frequency independent or frequency dependent.

Implementing the simplified method highly relies on the proper selection of required interaction parameters together with considerable engineering judgment and experience to get meaningful results. Approximate analytical techniques are usually used in practice to determine the parameters of a coupled structure/spring/dashpot system, such as weighted modal damping, lumped-mass sticks, soil springs, etc. A basic assumption of this method is that the response of the structure has no significant impact on the free ground motion as a result of the interaction. This method reasonably incorporates the kinematic interaction effects by simplified discrete approaches, and has been widely applied in Japanese nuclear engineering to predict the effects of seismic SSI.

Roesset [1989] discusses the differences between direct and sub-structure approaches. The direct approach by definition solves the seismic response of a structural system in a single step by presenting the structure and surrounding soil media together in a combined model. This one-step method can directly compute the seismic stresses in the

60

structural components utilizing complete analytical techniques corresponding to different models. This rigorous solution, however, requires a full-scale 3D description for the configuration of the overall soil-structural system and an appropriate nonlinear constitutive model, which significantly increases computational efforts. In practical application, the compatible motions and stresses on the boundaries of the soil domain can be determined first to simplify the analysis. This procedure is particularly attractive for true nonlinear analyses including the complete SSI effects. However, to simplify the complexities and uncertainties, the nonlinear soil behavior is usually simulated using equivalent linearization.

As an alternative to the direct solution, the overall soil-structural system can be handled by the sub-structure (impedance) approach, which divides the entire system into a series of simpler sub-systems and solves the associated sub-problems successively by the multistep method. As noted previously, these sub-problems include the site response problem, the scattering problem, the impedance problem, and the structural response problem. The involved multistep method calculates the initial results in the first step and utilizes these results as inputs to subsequent steps. The model for the first step is required to represent the dynamic behavior of the whole system but need not be refined to predict stresses in individual building components. A lumped-mass parameter model is acceptable for this step. The scattering problem can be avoided by explicitly modeling the embedment in the free field utilizing certain algorithm manipulations, such as the flexible volume and subtraction methods implemented in SASSI (Lysmer et al. [1999]).

Most available computer codes based on the sub-structure approach are developed in the frequency domain. Because of the implicit use of the superposition principle, the sub-structure solution is limited mainly to linear elastic problems, although it is possible to perform nonlinear analyses if the solution is formulated in the time domain and the coupling between substructures is taken into account in each time step. Nevertheless, because of its clear definition and dissection of physical problems associated with the SSI phenomenon, the sub-structure solution is widely practiced in the engineering field for seismic analyses.

Nuclear facility buildings and components are often analyzed using the sub-structure approach in multiple steps because of the geometric complexity, the dimension of the system, as well as the jurisdictional responsibility of geotechnical engineers and structural engineers. The initial analysis usually starts with investigating SSI effects of the global system, which primarily consists of the detailed soil model coupled with a simplified structural model (e.g. lumped-mass stick). The structural model used herein does not necessarily have sufficient details to predict stresses accurately at this stage, since only the response acceleration and displacements are needed for the subsequent analyses. The generated ground motions in this step are then provided to a complete structural analysis model (excluding the soil media) for further spectrum or time history analyses of the structural responses. Usually, the design seismic stresses and floor response can be obtained in this stage for subsequent evaluation of other components such as piping, equipment, and secondary structural components.

3.4   EXPERIMENTAL REVIEW

Abundant experimental data utilizing earthquake simulation techniques such as explosions and shaking table tests are available in the historic records to help better understand the dynamic response of structures and soils in real earthquake events. They can also be used to verify and validate analytical techniques or methodologies for calculating the seismic responses of a soil-structural system. Particularly in nuclear engineering field, EPRI and NRC sponsored a series of in-situ dynamic tests since the 1980s using scaled models of nuclear containment buildings (e.g., Simquake I, II & III, or Lotung & Hualien project, etc.) in order to investigate and better understand the seismic behaviors of NPP safety related structures. Valuable information was obtained from these field tests. However, due to scaling limitations, the experimental results can only be used for parameter identification and method verification rather than for direct application to prototype structures in an actual earthquake environment. So far, testing on full-scale structures subjected to a simulated earthquake cannot be performed because methods to shake the structure at appropriate energy levels have not been developed. As an alternate, most physical reactor buildings globally have installed seismometers in order to collect first-hand response data from any actual earthquake events.

This section presents a brief review on some of the recorded data, together with discussions on the seismic SSI effects.

3.4.1   Simquake II (EPRI [1981])

Simquake II experiment, which was conducted by the University of New Mexico at its McCormick Ranch test site in October, 1978, includes a series of field tests utilizing high energy explosions to simulate seismic ground motions striking on containment buildings. The purpose of this study was to obtain experimental evidences to assist the EPRI to validate analytical methodologies and to set up engineering guidelines for analyzing SSI effects. In parallel, Simquake II provided an opportunity to investigate in-situ techniques for the determination of dynamic soil properties at high-strain levels, to produce a database for simulation of earthquake ground motions, and to test the base isolation using engineered rubber supports.

Six cylindrical testing models were constructed with scale factors varying from 1/48 to 1/8 of a full-size containment building. The largest model was 4.6 m (15 ft) in diameter, 6.9 m (22.5 ft) high, and embedded to 25% of the height in native soil backfill. The shear velocity of the soil measured in field within the top 27.4 m (90 ft) of the ground varied from 244 m/s to 335 m/s (800 ft/s to 1100 ft/s). The ground water table at the test site was below 91.4 m (300 ft). The oscillating forces were generated from two buried explosive arrays located about 61.0 m (200 ft) away from the structural models. The nominal array size was 61.0 m (200 ft) wide by 22.9 m (75 ft) deep, leading to an average loading density of 0.15 kN TNT/m^2 (3.26 lb TNT/ft^2). The front array was designed to be delayed about 1.2 seconds after the back array detonated. These double-array detonations with time delay created about four significant cycles of horizontal soil velocity. The time duration of excitation lasted about 2.5 seconds. It was recognized that the wave types

caused by explosions are different from those caused by earthquakes. This is because the ground motion induced by explosion is primarily generated by compression wave, although there are significant motions associated with shear wave, especially in the near-surface area.

Various transducers corresponding to a total number of 145 instrument channels were installed in the free field and in the structures. The measurements on the structures included additional angular displacement and interface stresses with pressure gages installed at the soil-structure interface, while the free field measurements consisted of three dimensional accelerations and velocities. The peak horizontal ground motions were found to be 2.2 g (acceleration), 0.95 m/s (velocity) and 0.14 m (displacement), respectively. However, the vertical velocity and displacement were found to be about one-half of the horizontal values, while the vertical acceleration was about 75% greater than that in horizontal. The major frequency was monitored within the range of 1 Hz to 2 Hz. The collected ground motions and interface pressures were utilized to evaluate the effect of structure size, embedment, the amplitude of motion, and the number of motion cycles as well as the rocking amplitude and frequency

According to the collected test data, all six structural models in this study exhibited strong nonlinear rocking behavior, which was evidenced by the measured rocking-ringdown frequencies, which were as low as 25% to 35% of the pre-test low-strain frequencies measured in a forced-vibration test. Further data analysis indicated that the nonlinear rocking response was induced most likely by the large ground motion amplitudes that lead to significant nonlinear soil strains due to the decrease in soil

stiffness and the gap formation (debonding-rebonding effects) at the soil-structure interface. The stiffening effect of embedment was also reduced substantially by the gap formation. In addition, the rocking amplitudes of embedded structures were found about 50% to 75% greater than those of structures on the ground surface. The rocking amplitudes were also affected by the type of backfill soil. More specifically, the amplitudes of sand backfilled structures were three times greater than those of structures in native backfill.

It was concluded from the Simquake II experiments that the phenomena associated with the reduction in fundamental rocking frequency could potentially have significant influence on prototype containment responses during an actual earthquake. It could most likely reduce the motion of the internal equipment owing to earthquake, but potentially increase soil pressures and displacement to the containment building itself.

3.4.2 Simquake III (EPRI [1988])

Niagara Mohawk Power Corporation (NMPC) cosponsored Simquake III field tests with EPRI at a site near its Nine Mile Point Plant (NMPP) to investigate a particular SSI case simulating the NPP structures founded in backfilled rock socket. In general, this type of construction provides a space between the exterior walls and the excavation of the rock socket, backfilled with a free-drained compressible material that may potentially respond as a seismic damper to dissipate more energy and reduce the dynamic loads imposed onto the structure. However, the effectiveness of this design had to be confirmed

and proven by tests or appropriate SSI analysis for the purpose of USNRC licensing review.

The project team constructed four reinforced concrete model structures with rock-socketed foundations, two of which were in a rectangular shape in 1/10 and 1/20 scales, and the other two in cylindrical shape with the same 1/12scale factor. Three planar arrays were sequentially detonated to create an earthquake-like ground motion input for the test structures. The structures and surrounding rock were instrumented so that both the ground motions and the corresponding responses of the structures were obtained. The data were later used verify the numerical methods used to simulate the seismic response of the system.

A total of 120 data channels were obtained from the explosion test, including acceleration, displacement and interface pressure in both the test structures and surrounding rock media. In addition, a total number of 106 forced-vibration tests using a hydraulic shaker were carried out to investigate the system frequencies and damping values before and after the explosions. The response of the explosion test was also monitored by tri-axial accelerometers installed near and inside NMPP Unit 1 located approximately 1219 m (4000 ft) from the explosion. These measurements were useful for assessing the dynamic properties of the actual plant to a low-level ground motion input.

According to the collected data, all testing models exhibited the nonlinear dynamic response with a 5-10% downshift in fundamental frequency when the force amplitude was increased. This value is much less than that measured in Simquake II tests

on a soft soil site. However, the degree of downshift clearly demonstrated the tested structure's nonlinearity. Compared with 3.5% to 7% damping from forced-vibration tests, the explosive test yielded a higher structural damping of 10%. This significant variation indicated that an important mechanism of energy dissipation exists in structural system.

However, it was observed that the backfills in sockets did not significantly influence the structural dynamic response (e.g., natural frequencies, damping values) even though the strain in the backfill extended to non-linear regime. This result deviated from predictions prior to field tests. Moreover, the natural frequencies of the cylindrical structures with backfills decreased rather than increased as predicted by a linear seismic analysis. According to the tri-axial acceleration time histories recorded at the NMPP Unit one containment building, at the peak ground motion of 0.01g, the damping was estimated as 8%, which is twice the 4% value as specified by NRC RG 1.60 for concrete structures.

Since the Simquake experiments could not accurately produce proper scaling and waveforms, the test results were recommended to be used for parameter identification or method qualification rather than for direct application to prototype structures in an actual earthquake environment. On the other hand, the Simquake tests confirmed that a nonlinear elastic model is more suitable for seismic response analyses of structures when the soil-structure interaction is taken into account.

3.4.3   Lotung Large-Scale Seismic Test (LSST) (EPRI [1987])

In cooperation with Taiwan Power Company (TPC), EPRI constructed the Lotung LSST facility in Taiwan to collect forced vibration and earthquake response data that would be used to validate existing methods for SSI analyses and facilitate future research. The Lotung site is located in a seismically active region within the southwest quadrant of the Strong Motion Array (SMART I & II in Taiwan), which were deployed by U.C. Berkeley under a U.S. National Science Foundation grant. Since its operation in 1985, more than 30 strong motion earthquakes ranging from Richter magnitude 4.5 to 7.0 have been recorded at this site.

The LSST facility includes two models scaled to 1/4 and 1/12 of a NPP containment structure. The quarter-scaled model has a cylindrical shape with a 10.5 m diameter and is 15.25 m high. It is embedded about 4.6m below the ground . The soil at Lotung is relatively soft with an average shear wave velocity of 100 m/s. Extensive instrumentation was installed to record both structural and ground responses during actual earthquakes. The layout of instrumentation for ground motion measurement included three linear surface arrays radiating about 47 m centered with the quarter-scale model, and two downhole arrays extending about 47 m below grade. A set of tri-axial force-balance accelerometers oriented in E-W, N-S and vertical directions were installed along each surface or downhole array. Both structural models were instrumented with tri-axial accelerometers as well. The accelerometers were approximately 50 Hz in natural frequency with 70% of critical damping ratio, and had a sensitivity of 1.25 volts/g within a full-scale of ±2 g. In addition, thirteen pressure-cell transducers, with the capacity of

1035 kPa and resolution of about 7 kPa were installed on the quarter-scale model to measure dynamic pressures at the soil and structure interfaces. Data recording started when the seismic trigger detected a ground motion above 0.01 g. All collected data from accelerometers and pressure transducers were processed by a data acquisition system using a computer program.

The Lotung LSST successfully produced a unique earthquake database for validating methods for seismic analysis and modeling techniques. Using this database, prediction and correlation studies have been performed to provide a basis to evaluate and qualify the seismic SSI analysis methodologies. A total of 13 research organizations and institutes all over the world participated in the experiments, and made blind predictions and comparisons with the measured earthquake responses. The analysis phase of the research was conducted with the cooperation of the U.S. NRC and TPC. A workshop was held in December 1987 where research results and findings were presented. Further effort is ongoing to synthesize the results and findings for providing technical bases of developing improved SSI analyses guidelines and procedures.

4 FEM MODEL FOR SEISMIC ANALYSIS

4.1 INTRODUCTION

In order to investigate the seismic-induced soil pressures and verify if existing methods as described in Sections 3.2 and 3.3 are applicable in the nuclear engineering field, a simplified CANDU 6 reactor building is selected as the sample case for fulfilling this project's objectives. CANDU 6 is the second generation of CANDU technology developed in Canada and has been proven by its reliable performance records around the world. A total of eleven (11) units are in operation in Canada and worldwide.

CANDU 6 is based on standardized design incorporating and enveloping a wide range of most severe field conditions to satisfy global markets. One major concern regarding the site selection is the geological information and associated parameters for assessing the potential seismic excitation. The standard CANDU 6 design is seismically qualified to Design Basis Earthquake (DBE) whose design ground response spectra are defined by CAN/CSA-N289 Standard series. Unfortunately, one of the important seismic design factors, the seismic-induced soil pressure, is not properly addressed in the standard design. This Chapter intends to use state-of-the-art analysis methods to determine the seismic-induced earth pressure by taking into account the effect of SSI for the design of the next generation ACR-1000.

4.2   DESCRIPTION OF THE SAMPLE FACILITY

A reactor building can be physically separated into two structural entities including the containment structure and the internal structure. The containment structure houses the nuclear reactor with associated safety-related systems and components directly supported by the internal structure. Figure 4-1 illustrates the general arrangement of the CANDU 6 Reactor Building in a 3D cutaway view.

The overall building size is determined by the equipment layout and the free building volume required to keep the accident pressure within a reasonable range. The thicknesses of the wall and the dome are determined primarily by the shielding requirements. To make the structure leak tight, the whole body of the containment building is pre-stressed to control tensile stress on the inside face of the containment boundary to keep it crack free and thus forms restraint against leakage. Consequently, it is reasonable to consider the concrete material to be linear elastic.

The perimeter wall is a 1.22 m thick by 54.86 m high cylindrical concrete shell. The inside diameter of the cylinder is 38.71 m. The perimeter wall is prestressed with 147 - 37 strand horizontal tendons and 124 - 55 strand vertical tendons. Tendon spacing is approximately one meter center-to-center. The wall is constructed continually using the slip-forming operation to avoid any construction joints, which in turn, enhances the leak tightness of the wall. The top of the perimeter wall is enlarged forming a ring beam about 2.1 m wide by 4.5 m high. The function of the ring beam is to house the prestressed

tendon anchorages and to resist significant forces due to discontinuity at the joint of wall and dome.
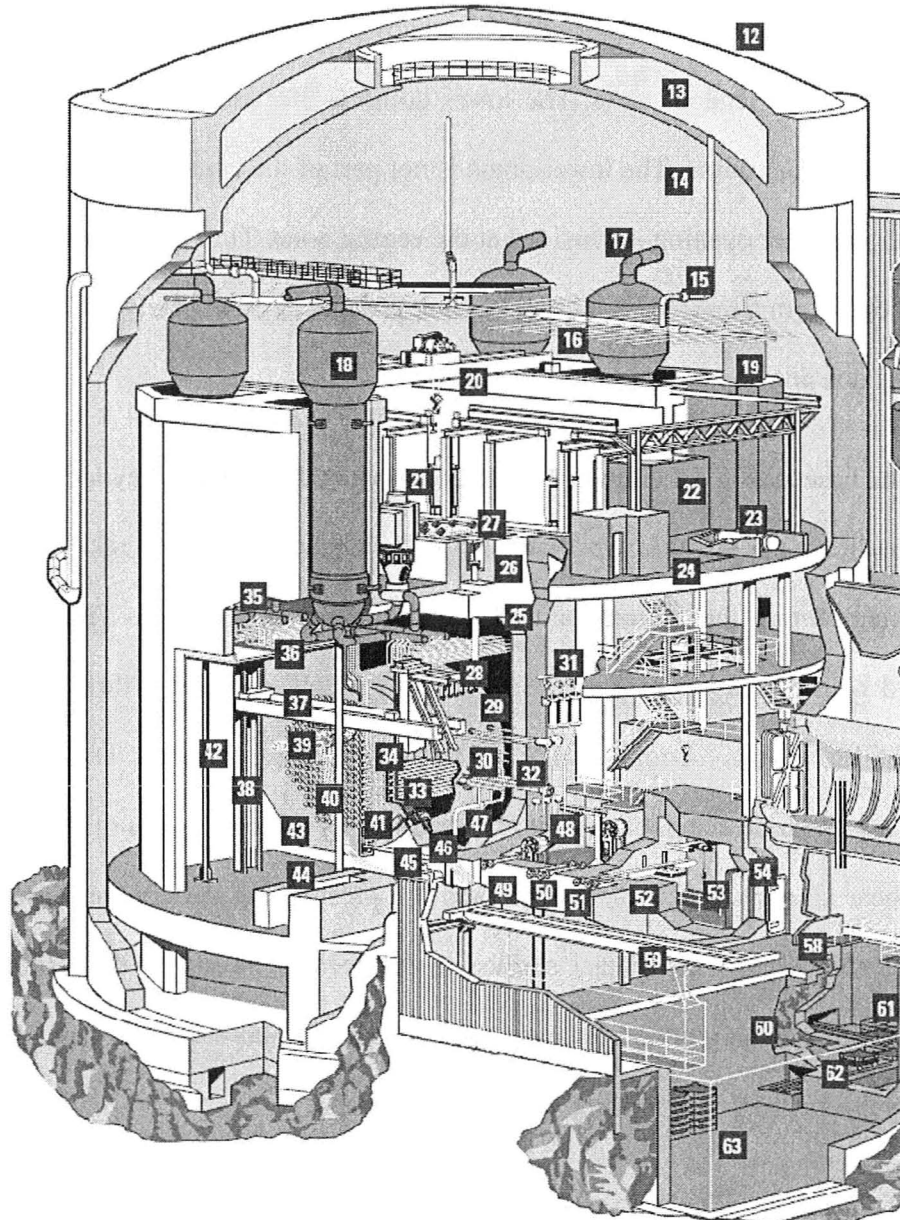

Figure 4-1: Cutaway of CANDU 6 Reactor Building (AECL [2005])

The containment roof consists of an upper dome and a lower dome, which are formed in a segment of a sphere with an inside radius of 38.71 m. The upper dome is 610 mm thick at center, and gradually thickened to about 1.25 m at the ring beam. The upper dome is prestressed with one layer of three groups of tendons at 120° apart, with a total of 141 - 37 strand tendons used. The lower dome is 380 mm thick and about 2.44 m underside the upper dome. The lower dome is not part of the containment boundary since a 10 meter diameter opening is provided at the central zone. The two domes together with the ring beam form a reservoir (dousing tank) to provide approximately 2,170 m^3 of water storage for dousing and emergency core cooling.

The base slab is a 1.83 m thick mat and projected about 2 m beyond the perimeter wall to distribute the pressure. The base slab is founded on competent rock or stiff soil as required and forms the bottom part of the containment envelope. The base slab is reinforced with two layers of prestressing tendons. Each consists of three (3) groups of tendons at 120° apart. A total of 126 - 55 strand tendons are used. To transfer lateral shear forces, the base slab is keyed into the bedrock by three (3) types of shear keys: one central shear key, six radial shear keys, and the prestressing gallery functioning as the peripheral shear key. The contact surface in between is inserted with a thin layer of sliding membrane. An under-drainage system under the sub-base eliminates the effects caused by the external hydrostatic pressure.

The internal structure has five (5) major concrete floor slabs supported by the concrete walls and columns at elevations 100.00 m, 107.93 m, 112.50 m, 115.55 m and 117.45 m. The overall mass center is not aligned with the rigidity center due to the

irregular floor layout arrangements. This geometric eccentricity will cause significant torsional effects under the seismic. The internal structure is anchored to base slab with dowels while its superstructure is separated with the exterior containment structure to simplify the interaction between the two structures.

Since this project focuses the discussions on the seismic-induced soil pressures applied onto the perimeter walls, the effects due to the co-response with internal structure are neglected. The structure is simplified by presenting the configuration of containment building only. However, its mass is lumped to the roof and base slab for determining the natural frequency of the overall structural system.

4.3   ANSYS ANALYSIS SOFTWARE

ANSYS software is used in this study for perform the seismic analysis of the soil-structure system. Developed by ANSYS Inc., ANSYS is a large-scale, general-purpose finite element computer program that utilizes incremental techniques for solving a wide variety of structural and geotechnical problems. As the only qualified software certified and accepted by NRC and CNSC, ANSYS has been adopted by most consulting firms and is extensively used in the nuclear engineering field since the 1970s.

ANSYS has tremendous capabilities for both static and dynamic structural analyses in association with the linear elastic, nonlinear and inelastic behaviors, steady-state or transient problems. The nonlinearities, which can be handled by the program,

include material plasticity, stress stiffening, large deflection or deformation, hyper-elasticity, interface contacts, and so on. Several typical analytical methods and techniques available in ANSYS are summarized below:

1. Static analysis is used to determine displacements, stresses, strains and forces under steady loading conditions, and ignores significant inertia and damping effects. All types of nonlinearities are allowed.

2. Modal analysis, which is linear, is used to determine the free vibration characteristics (i.e., the natural frequencies and the mode shapes) of a structural system. Any pre-defined nonlinear properties are ignored.

3. Transient dynamic (time-history) analysis is used to determine the dynamic response of a structure under the action of any arbitrarily time-dependent loads. It also allows all types of nonlinearities. The inertia and damping effects are important.

4. Spectrum analysis is an extension of the modal analysis replacing a time-history analysis with its frequency response equivalent to determine the response of structures, and used to calculate stresses and strains, or displacements due to a response spectrum or a PSD input for random vibrations. Only linear behavior is valid.

The ANSYS program provides a large library of element types applicable for both 2D and 3D model analysis. The degrees of freedom (DOF) are assigned to each particular element to constitute the primary unknowns. Proper selection of element types with

appropriate DOF can effectively balance the solution requirements and the amount of computing work that determines the time required to complete the analysis.

ANSYS also has a comprehensive material library. Depending on the nature of the problem to be solve, various material properties, including modulus of elasticity and rigidity, Poisson's ratio, damping, thermal coefficient among many others can be assigned to different elements to represent varying material characteristics such as linearity or nonlinearity, isotropy or anisotropy, elastic or elasto-plastic, time-independent or time-dependent behavior. The program also provides flexibility allowing users to create elements and to define particular material properties based on their specific needs.

ANSYS Workbench, which represents the new-generation solution from ANSYS, provides powerful methods for interacting with traditional ANSYS solver functionality. Moreover, it provides a complete environment for geometry modeling, mesh manipulation, structural analysis, and optimization, which is tightly integrated with a CAD system and analysis process. Its friendly interface allows a user to create complex structural models to simulate the soil-structure interaction rapidly and in details by taking into account nonlinear materials, varying geometry and contact conditions as well as different designs for the structural elements of the project. The Workbench package consists of five functional components, including design module, CFX mesh, Finite Element module, simulation, and design Xplorer. The latest version (12.0) includes enhancements for structural modeling and dynamic analyses, with automated and convenient meshing tools to simplify the mesh generation process. Owing to its

considerable advantages, ANSYS Workbench 12.0 is selected as the analysis tool for case study in this project.

4.4 MODEL DESCRIPTIONS

A simplified CANDU containment building is modeled herein using the ANSYS to evaluate seismic-induced soil pressures in accordance with different analytical methodologies as described in previous sections. The overall geometry of the structural model follows the physical arrangement of a real CANDU containment building. The profile and general arrangement of the simplified model is sketched in Figure 4-2.
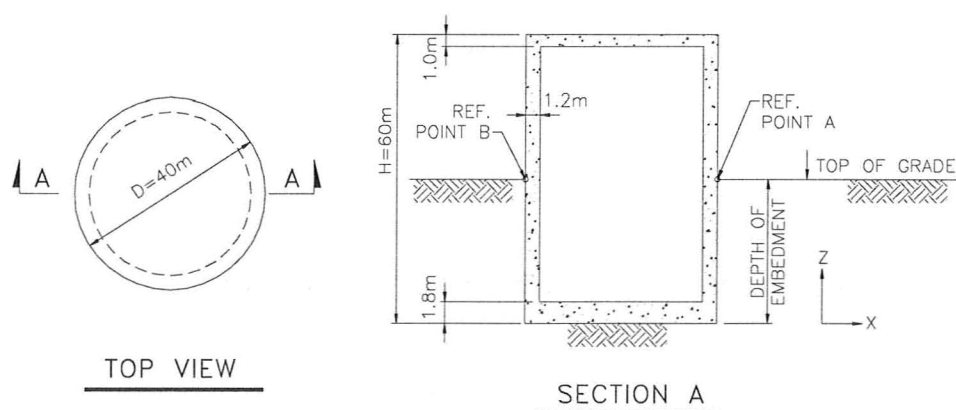

Figure 4-2: General Arrangement of Simplified Analysis Model

The rigid cylindrical concrete structure is 40 m in diameter and 60 m in height. The thickness of its wall and base slab is 1.2 m and 1.8 m, respectively. The selection of the wall thickness considers the equivalent moment of inertia with the combination of exterior concrete wall and attached steel liner plates. The area of cylindrical cross section is 146.3 m^2. The corresponding moment of inertia is calculated as 27,550 m^4. Instead of modeling a dome shape, the roof is simplified as a flat roof with a uniform thickness of 1.0 m. This simplification is assumed to have insignificant influence on modelling the soil-structure interaction since the roof is above the ground surface, as shown in Figure 4-2. Stiffness effects due to the internal structure are not included in this analysis model. However, their mass is lumped to the roof and base slab, respectively. The total weight of the structure has been adjusted when comparing it with a real containment building to obtain structural frequencies that are likely to be interactive with the whole SSI system.

Traditionally, the containment buildings are constructed with shallow embedment (approximately 1/5 of the building height). For this case study, in order to investigate the significant kinematic effects due to embedment variation, the model is partially embedded below the grade, with two case scenarios corresponding to embedment depth as a quarter or a half of the building height of the structural model. The schematic 3D view of the ANSYS model with the structure half embedded is shown in Figure 4-3. The model is placed in a global Cartesian coordinate system whose origin is set at the center of the structure's bottom base slab. The X and Y directions represent two principle orthogonal axes in the horizontal direction, while the corresponding Z axis is in the vertical direction. A local cylindrical coordinate system is used to facilitate extracting and post-processing

the output data. Considering the symmetric characteristic in geometry, applied loading and boundary conditions, only a half of the model section is used in the numerical analysis to save computing time. It should be noted that the X-Z plane through the origin is defined as the plane of symmetry. Even though varying element mesh sizes result in different system stiffness and hence different frequency characteristics in different regions, this effect is considered as negligible according to the past experiences.
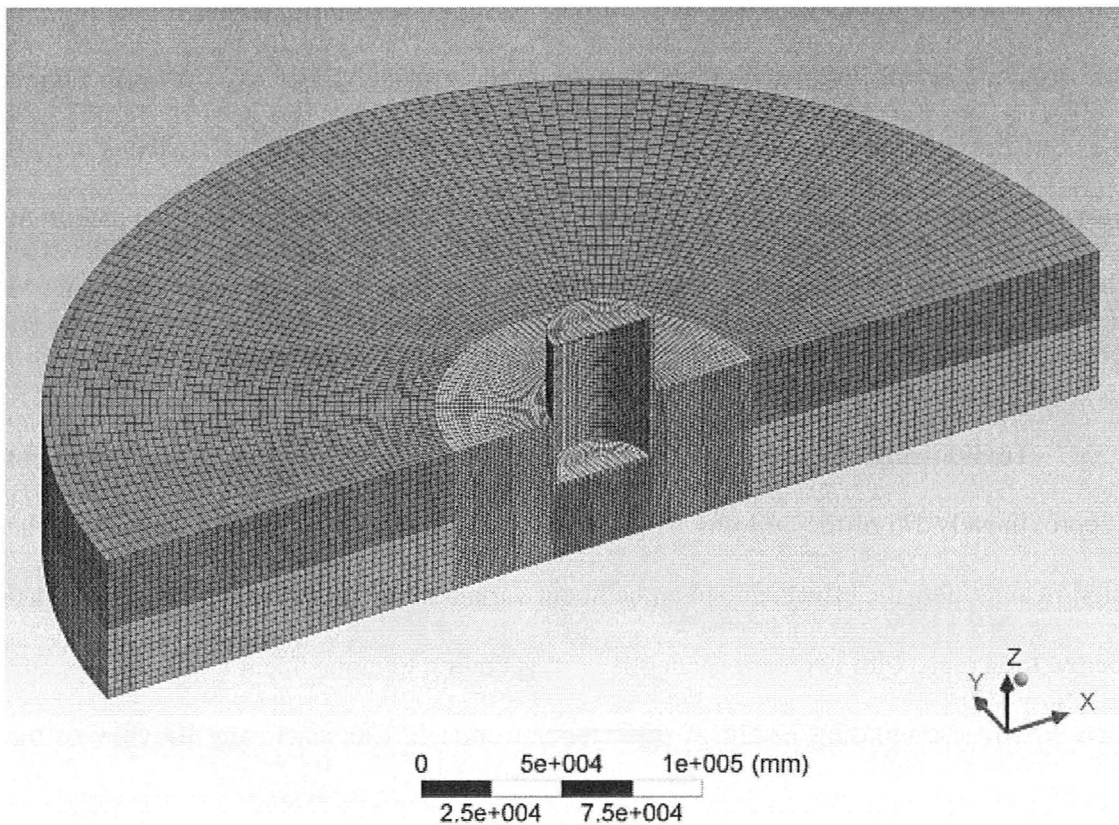
Figure 4-3: 3D View of FE Analysis Model with Half Embedment by ANSYS

The boundaries of the soil media are located about 200 m away from the center of the structure. In addition, the boundary is laterally restrained by a series of viscous dashpots in order to absorb wave energy and minimize potential effects caused by the reflections of input seismic motion. Moreover, the viscous boundary is considered to be independent of the frequency. The FEM model includes two layers of soil: a layer of stiff soil below the base slab of structure and a relatively soft soil layer on the top. The stiff soil layer sits on the bedrock, which is stimulated by a pre-defined seismic motion. In order to study the effects due to soil nonlinearity, adjacent to the building structure, a 40 m wide immediate area is defined as a near field zone, which is meshed with a finer element size. Regions at far field, which are of less interest, and hence are discretized by relatively coarse meshes.

The FEM model consists of 200,785 nodes and 176,688 solid elements in total. Eight-node 3D solid elements SOLID65 and SOLID185 are selected for modeling concrete and soil, respectively. Particularly, the SOLID185 element has plasticity, hyper-elasticity, stress stiffening, large deflection, and large strain capabilities. It also has mixed formulation capabilities to simulate nearly incompressible deformations of elasto-plastic materials, and fully incompressible hyper-elastic materials. The SOLID65 element is used for the 3-D modeling of reinforced concrete with or without reinforcing bars (rebar). The solid is capable of cracking in tension and crushing in compression.

In order to simulate the contact condition at the soil-structure interface, two types of interaction boundaries, which can be fully bounded or separated, are used in the model. The bonded interface glues the solid bodies at the contact surface without sliding or

separation occurring in between. Any potential gaps are closed and any initial penetration are ignored. As such, this type of contact allows for a linear solution since the contact area does not change during the load application. In this case, the soil-structural elements at the interface boundary deforms together and have identical responses. At the interface boundary, however, occurrence of element separation or penetration from each other is permitted. Element separation and penetration is typically non-linear, which may induce severe numerical difficulties. Theoretically, the contact behavior is controlled by the contact stiffness. Higher stiffness values reduce the amount of penetration, but could lead to ill-conditioning of the global stiffness matrix and cause convergence difficulties. On the other hand, lower stiffness values tend to be well-behaved in terms of convergence and generate a certain amount of penetration with longer computing times; however this may produce an inaccurate solution. Traditionally, this kind of separation behavior is usually simplified or even neglected, which is acceptable, since separation is less important for shallow embedded facilities. With the increase of embedment depths, separation between the structure and soil tends to have significant effect on the determination of the seismic-induced soil pressures. Considering the nature of the soil-structure interaction in this study, a frictional contact is selected to simulate the relative deformation between the contacting bodies and predict the nonlinear behavior due to a slight separation or penetration at the contact interface between soil and the structure. In ANSYS, the interface is described by a pair of rigid-flexible contacts comprising a target surface and a contact surface. The contact elements are constrained against penetrating the target surface. However, target elements can penetrate through the contact surface.

Since the soil elements are more deformable and less rigidity than the concrete elements, the surface on the concrete side is defined as the target surface using element TARGE170 while the soil side boundary is designated as the contact surface using element CONTA173 in ANSYS.

4.5   ASSUMPTIONS AND CONDITIONS

To simplify the analysis and verification work in this project, the following assumptions are made for model analysis and be comparable with the static solutions:

1. A perfect bonding exists between the structure and the sub-base soil. No separation at this interface boundary is expected to take place during seismic excitation.

2. The movement and the corresponding frequency range of the internal structure and supporting system for major equipment are not considered in numerical modeling. In other words, any influence of the internal structures is neglected.

3. Any potential interaction effects from adjacent structures are neglected.

4. The seismic analysis does not combine with other service live loads or environmental loads except as specified in Section 4.6.1.

5. Seismic motion is applied in one principal horizontal direction only.

6. Drained conditions are assumed. Pore pressure and any associated hydrodynamic effects under strong earthquake motion are neglected.

7. Torsional effects due to geometric and accidental eccentricities are ignored.

8. Damping and sloshing effects due to the water tank in the roof are not included in the consideration.

9. No strain hardening and associated progressive yielding of either concrete or soil are expected.

4.6   INPUT DATA

4.6.1   Material Properties

As described in the previous section, the FEM model includes three types of materials: i.e., concrete, soil media and bedrock. The standard reinforced concrete used for the structural model meets the requirement of CSA Standard CAN/CSA – A23.1/A23.2, and the material properties are summarized in Table 3.

Since the nonlinearity is expected to be extremely important in determining SSI responses and the seismic soil pressures under a strong ground motion. The Drucker-Prager (D-P) model with no strain hardening is selected as the constitutive model for soils. Table 4 summaries the mechanical properties of the soils used in the analyses.

Table 3: Material Properties – Concrete

Material Properties	Reinforced Concrete
1. Unit Weight (γ_c)	23.5 kN/m^3
2. Specified Compressive Strength (f_c')	35 MPa
3. Modulus of Elasticity (E_c)	28,165 MPa
4. Poisson's Ratio (ν_c)	0.2
5. Critical Damping (β_c)	3 %

Table 4: Material Properties – Soils

Material Properties	Surface Soil	Sub-Base Soil
1. Unit Weight (γ_s)	18 kN/m^3	20 kN/m^3
2. Constrained Elastic Modulus (E_s)	462 MPa	3211.6 MPa
3. Shear Modulus (G_s)	165 MPa	1147 MPa
4. Shear Wave Velocity (V_s)	300 m/sec.	750 m/sec.
5. Poisson's Ratio (ν_s)	0.4	0.4
6. Critical Damping (β_s)	7%	5%
7. Friction Angle (ϕ_s)	35°	35°

In order to investigate the effects of material nonlinearity on soil-structure interaction, the DP model for the soils is also used to simulate the nonlinear response

together with either contact or bounded interfaces, particularly for the structure with half embedment. However, to simplify the analysis process, only soil elements at the near field zone are assigned with nonlinear characteristics.

The bedrock is considered as visco-elastic with a shear wave velocity of 1500 m/sec, which corresponds to the shear modulus of 5,045 MPa. The damping ratio and the unit weight of bedrock are chosen as 2% and 24 kN/m^3, respectively.

4.6.2   Input Ground Motions

In general, the time-history accelerograms used for a seismic analysis is either selected from an appropriate recording of past strong motions or artificially synthesized ground motion. Then its amplitudes and frequency content are scaled such that the modified ground time-histories are compatible with CSA-based design ground response spectra as described in Section 2.1.2.

For the study in this project, one of the artificial time-histories developed by AECL for a generic rock site is utilized as the input ground motion. This artificial time-history is generated based on the superposition of sinusoids with random phase angles and amplitudes derived from a stationary power spectral density function of the motion. The input parameters for such ground motion are the sinusoidal amplitudes and phase angles, which participate as the characteristics of the motion intensity varying in time, especially the motion duration.

The procedure to generate AECL artificial time-histories is briefly described as follows. A series of motion records were first compiled including some modified rock-like records from several seismic active regions. These records are then used as input to an algorithm that modifies the input motion in the spectral domain by enhancing amplitudes at some frequencies while suppressing amplitudes at the others, such that the spectral content of the modified record matches the target spectrum (i.e., the rock outcrop motion anchors at 0.3 g). A key advantage of this technique is that phase characteristics of the record are not modified, and thus it retains the character of the original earthquake time-history.

This seismic input motion for a typical rock site is expressed as an acceleration time history and illustrated in Figure 4-4. The seismic motion is excited at the bedrock outcrop and applied in one principle horizontal direction only. The data points in the history table are at equal time spacing of 0.01 sec. with the first value starting at t = 0 sec.
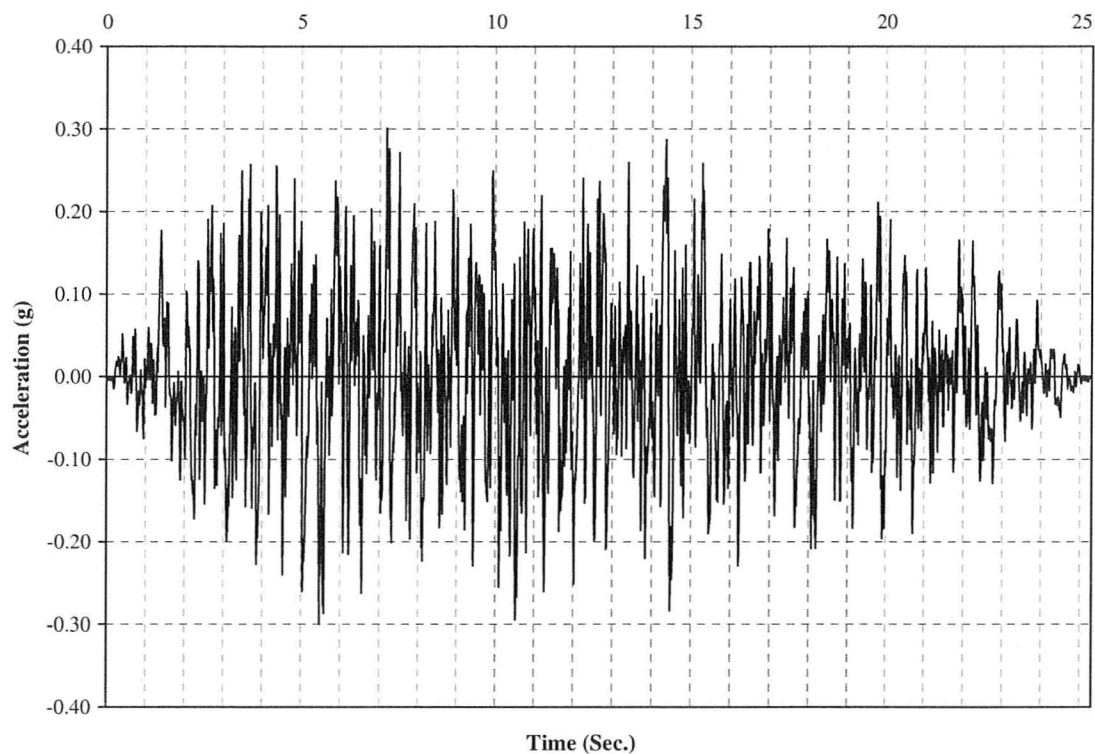
Figure 4-4: Acceleration Time-History for a Rock Site (Developed by AECL)

5 COMPUTATION RESULTS AND DISCUSSIONS

5.1 INTRODUCTION

As discussed in Chapter 3, methods to determine the seismic-induced earth pressure can be grouped into two major categories: simplified pseudo-analytical methods and detailed FE analytical methods. The simplified methods are represented by either equivalent static or pseudo-dynamic approaches, which are straight forward and easy for implementation in engineering practice, but cannot appropriately address the effect of SSI. Consequently, the results are generally less accurate and may not be broadly applicable for different kinds of field conditions. The detailed dynamic methods, either linear or nonlinear, can produce more accurate and close to realistic solutions, but require tremendous computation efforts, especially when involving nonlinear issues including both material nonlinearity and contact behaviour at the interface.

In this section, various methods previously reviewed and discussed in Sections 3.2 and 3.3 are used to calculate the seismic-induced earth pressures for the particular nuclear facility described in Section 4.2. The methods examined in this Chapter include:

- Equivalent static methods: Yielding wall models (i.e., the M-O method, the method proposed by Koseki et al. [2007]), and rigid wall models (i.e., the models proposed by Wood [1973], Ostadan [2005] and Nukui [1989], respectively);

- Pseudo-dynamic analysis methods: The methods proposed by Wu and Finn [1999], Choudhury and Nimbalkar [2005], respectively.

- Detailed FEM using ANSYS

The results obtained from different methods are compared to identify which simplified method is more reasonable and suitable for engineering application, and how practical it is to perform a full dynamic analysis.

5.2   SIMPLIFIED ANALYTICAL APPROACHES

5.2.1   Per Equivalent Static Analysis

Five equivalent static analysis methods as discussed in Section 3.2 are utilized for this specific case study. Two of them, the M-O method and the method proposed by Koseki et al. [2007], are based on the yielding wall theory. The other three, proposed by Wood [1973], Ostadan [2005] and Nukui [1989], respectively, are based on the rigid wall theory. All of these methods are applicable for predicting active pressures. The M-O method also provides a similar solution to quantify the passive effects. The pressure

distributions over the embedded section of the wall are presented in Figure 5-1. To make results comparable, lateral active soil pressures are normalized values by the vertical geostatic stress γH in soil at the embedment depth. The general comparisons of results obtained from different models for different embedment depths are summarized in Table 5 and Table 6.
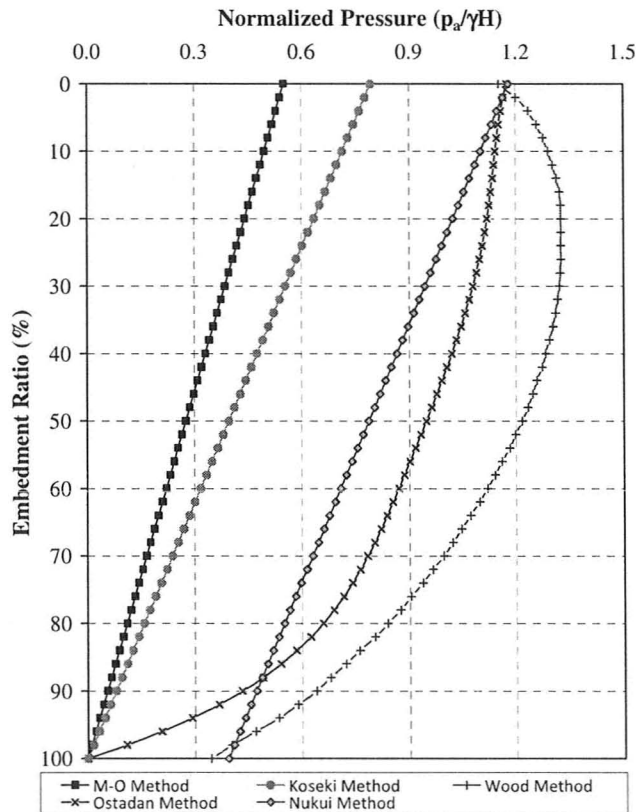

Figure 5-1: Lateral Pressures Based on Equivalent Static Analysis

Table 5: Result Comparisons for Equivalent Static Analysis with Quarter Embedment

Result Comparison (per Unit Width)	M-O Method	Koseki Method	Wood Method	Ostadan Method	Nukui Method
Total Thrust Force (kN/m)	1115	1605	4383	3516	3186
Thrust Location from Ground surface (m)	5	5	6.55	6.19	6.25
Maximum Pressure (kPa)	148.7	214.0	358.3	317.5	318.6
Max. Pressure Location from Ground Surface (m)	0	0	3.9	0	0
Minimum Pressure (kPa)	0	0	93.0	0	106.2
Min. Pressure Location from Ground Surface (m)	15	15	15	15	15

Table 6: Result Comparisons for Equivalent Static Analysis with Half Embedment

Result Comparison (per Unit Width)	M-O Method	Koseki Method	Wood Method	Ostadan Method	Nukui Method
Total Thrust Force (kN/m)	4461	6419	17530	14064	12511
Thrust Location from Ground surface (m)	10	10	13.1	12.38	12.5
Maximum Pressure (kPa)	297.4	427.9	716.6	635.0	625.5
Max. Pressure Location from Ground Surface (m)	0	0	7.8	0	0
Minimum Pressure (kPa)	0	0	186.0	0	208.5
Min. Pressure Location from Ground Surface (m)	30	30	30	30	30

As observed from Figure 5-1 and Tables 5 & 6, the active seismic earth pressure obtained from different methods may vary over a wide range, including both the amplitude of the total thrust force and the location at which the total force is applied. As the Koseki's method is derived directly from the M-O method with the effect of strain localization in soil behind the wall being taken into account, both of them have similar triangle distribution profiles varying from zero at the base to the maximum at the ground surface. However, pressures calculated by the Koseki's method are about 45% higher. This is not a surprise since the residual friction angle is used in the shear zone when determining the earth pressure using the Koseki's method.

As one might expect, the potential displacement of the wall has remarkable influence of seismic-induced earth pressure; as evidenced by the different earth pressures obtained from the yielding wall models and the rigid wall models shown in Figure 5-1 and Tables 5 & 6. In general, a rigid wall model predicts much higher seismic earth pressure than the yielding wall model. More specifically, Wood's method generates the highest pressures over the embedment with a curved distribution. The peak value is found at a location about 20% of embedded depth from the ground surface, and is about 2.4 times of the maximum value calculated by M-O method. The Ostadan's method incorporated the dynamic effects by introducing an adjustable factor varying with the Poisson's ratio of soil when determining the system's mass density. The pressures are distributed following the function as given in Equation 18. Different with Wood's method, the distribution by Ostadan's method has a relatively flat curvature with the zero pressure at the foundation base and the maximum located at the ground surface. Nukui's

method has a linear distribution with a shortcut to Wood's distribution curve. Unlike other three methods, Wood and Nukui's methods produce none-zero pressure at the foundation base and approximately one-third of the pressure at the ground surface.

Comparing the total lateral thrust forces, the methods following the rigid wall theory will have significantly higher values on average, approximately three times that of the ones predicted by the yielding wall theory. However, the rigid wall theory gives lower application position of the total thrust force than the yielding wall theory.

5.2.2   Per Pseudo-Dynamic Analysis

This section focuses on the discussion and comparisons of seismic earth pressure obtained from two models (Wu and Finn [1999], Choudhury and Nimbalkar [2005]) based on pseudo-dynamic analysis. Since the model by Wu and Finn [1999] was developed based on Wood's model, while the model by Choudhury and Nimbalkar [2005] was originated from the M-O method, some similarities are observed between these models. As shown in Figure 5-2, the results of the M-O method and the Choudhury method are similar, with the major difference at the upper half of the wall. It is also expected that the Choudhury method predicts smaller (approximately 25% smaller) earth pressure than the M-O method. The model developed by Wu and Finn [1999] is close to Wood's model at half embedment, but much higher earth pressure is obtained from Wu and Finn [1999] when the embedment is a quarter of the wall height. The computation results are also summarized in Table 7 & 8 for two different embedded cases (quarter and

half embedment, respectively) . To facilitate the comparisons, the results by the M-O and

Wood method are repeated in the figure and tables.
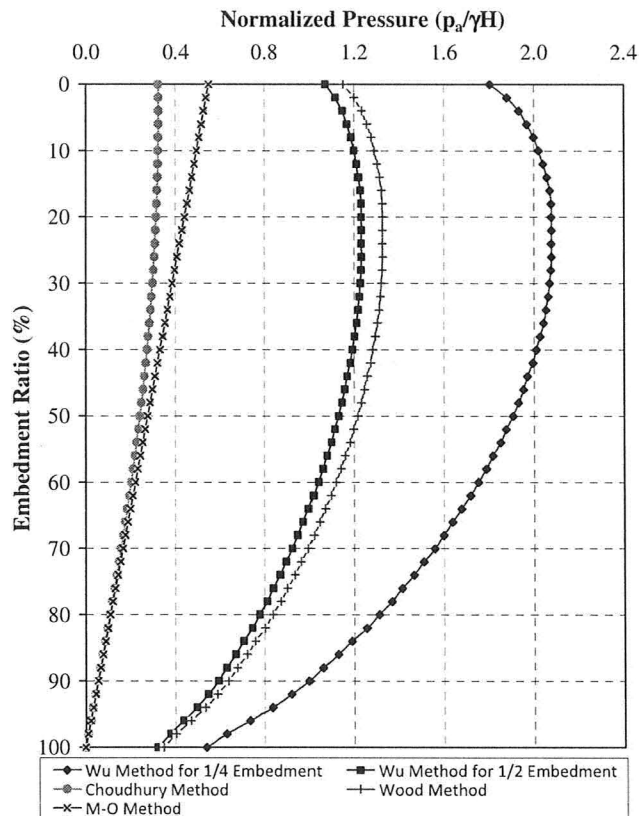
Normalized Pressure ($p_a/\gamma H$)

Figure 5-2: Lateral Pressures Based on Pseudo-Dynamic Analysis

The differences between the methods proposed by Wood [1973] and Wu & Finn

[1999] are summarized as follows. The method proposed by Wu & Finn [1999] considers

the amplification or reduction effect based on the different frequency ratio between

frequency of the excitation and the fundamental frequency of the wall-structure system

that varies with embedment depth. Consequently, the seismic pressure varies with embedment depth as shown in Figure 5-2. In addition, a set of factors adjustable for different damping and Poisson's ratio was also introduced by Wu & Finn [1999]. However, the Wu's method only provides the solution to determine the total lateral thrusts without specifying the corresponding pressure distribution. For the purpose of comparison, Figure 5-2 applied the same pressure distribution as proposed by Wood [1973] to present the results obtained from Wu's method. It is found that the Wu's method produces a slightly lower pressure (about 6%) for the half embedment case as compared with the Wood's solution. However, the pressure is largely amplified (about 50% higher) for the quarter embedment due to significant harmonic excitation.

Table 7: Result Comparisons for Pseudo-Dynamic Analysis with Quarter Embedment

Result Comparison (per Unit Width)	M-O Method	Wood Method	Pseudo-Dynamic	
			Wu Method	Choudhury Method
Total Thrust Force (kN/m)	1115	4383	6863	864.0
Thrust Location from Ground surface (m)	5	6.55	6.55	5.53
Maximum Pressure (kPa)	148.7	358.3	561.1	87.3
Max. Pressure Location from Ground Surface (m)	0	3.9	3.9	0
Minimum Pressure (kPa)	0	93.0	145.6	0
Min. Pressure Location from Ground Surface (m)	15	15	15	15

Table 8: Result Comparisons for Pseudo-Dynamic Analysis with Half Embedment

Result Comparison (per Unit Width)	M-O Method	Wood Method	Pseudo-Dynamic	
			Wu Method	Choudhury Method
Total Thrust Force (kN/m)	4461	17530	16294	3456
Thrust Location from Ground surface (m)	10	13.1	13.1	11.06
Maximum Pressure (kPa)	297.4	716.6	666.1	174.6
Max. Pressure Location from Ground Surface (m)	0	7.8	7.8	0
Minimum Pressure (kPa)	0	186.0	172.9	0
Min. Pressure Location from Ground Surface (m)	30	30	30	30

As discussed previously, only the M-O method and the Choudhury method propose solutions to determine the passive pressures. As shown in Figure 5-3, both methods unreasonably over-estimate the passive effect, and are not suitable and are not recommended for the engineering application.
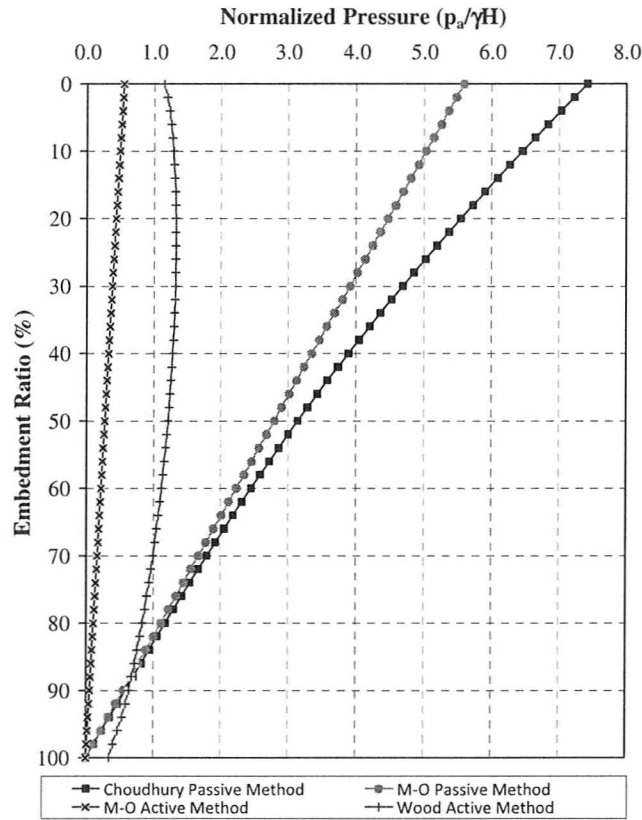
Normalized Pressure (p$_a$/γH)

Figure 5-3: Lateral Pressures Based on Passive Analysis

5.3 FE ANALYTICAL SOLUTIONS

A full transient dynamic analysis with the consideration of linear and nonlinear effects was performed by using ANSYS software to determine lateral soil pressures due to a strong ground motion. The 3D FEM seismic analysis was carried out using the model described in details in Section 4.4.

As discussed previously, seismic-induced soil pressures should be imposed by the combination of inertial and kinematic interaction effects. The inertial forces transferred from the superstructure are expected to be the major contribution to the movement of the underground structure and hence to the lateral soil pressures for shallow embedment. With an increase in embedment depths, however, the kinematic deformations of the underground walls gradually become more significant for seismic earth pressure. In order to understand the importance of embedment depth for effects associated to the inertial and kinematic interactions, two cases with embedment depth being a quarter or a half of building height are considered in the analysis.

In addition to the effect of embedment, two interface conditions (i.e., an ideal bonding interface and a frictional contact) are examined in the analysis to simulate SSI effects. More specifically, a frictional coefficient of 0.315, which corresponds to a 17.5° friction angle, is assigned at the contact interface to allow potential sliding and separations between the structural and soil elements. It should be noted that in the FE simulations, the distribution of lateral soil pressures is determined directly from the stresses of soil elements at the interface with the structural elements based on local cylindrical coordinate system.

To be consistent and make results comparable, the reference point is selected at Point A, which is located at the top interface corner and 0.75 m below the ground surface. See Figure 4-2 for its location. Moreover, an opposite Point B is also considered in comparisons for bonded interface condition considering its symmetric characteristic.

Except noted otherwise, the sign conventions for soil pressures are assigned as compression in negative and tensile stresses in positive.

5.3.1 Analysis with Bonded Interface

The first scenario for detailed finite element analysis considers the linear elastic material with an ideally bonded interface at the contact boundary. For this case, the material properties are independent of stresses and deformation histories.

(a) Quarter Embedment

For the quarter embedment, the variation of lateral soil pressures in an earthquake lasted for 20 seconds is illustrated in Figure 5-4. Herein the lateral earth pressure is the radial pressure in the direction in which the excitation is applied. At reference Point A, two peak values, 377.87 kPa and -371.07 kPa, are observed at 9.02 second and 12.44 second, respectively. The first peak pressure appears after the input acceleration of motion reaches 0.3 g at 7.19 second. The second peak value occurs when the acceleration of motion is about 0.295 g at 10.52 second. It has been noticed that the corresponding response at the top of structure is excited more than 0.9 g.

At the moment when the first pressure peak appears, the distributions of lateral pressure against depth at both Point A & B, which is expressed as the nominal embedment ratio, is presented in Figure 5-5. Very high soil pressure distributes within the top 30% of the embedded structure. The soil pressure at the middle 30% to 70% of the wall height is almost constant, with the average being about 66 kPa. The soil pressure

attenuates rapidly beyond the 70% embedment and reaches to zero at the foundation base level. Compared with the soil pressure distributions obtained from simplified procedures (see Figure 5-1 and Figure 5-2), one observes that the FEM seismic analysis yields much higher earth pressure at the top 30% of the wall. The high lateral pressures near the ground surface are resulted from the inertial forces transferred from the super-structure due to the overturning effects.
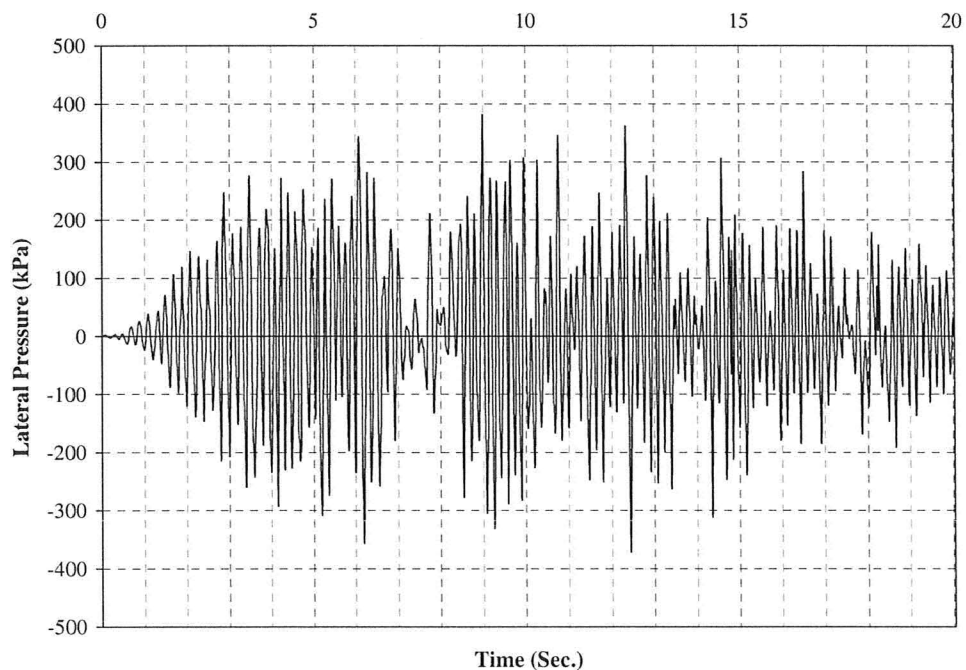

Figure 5-4: Pressure Time History at Point A for Bonded Interface for

Quarter Embedment

When superposing the seismic earth pressure response onto the static one, the negative total earth pressures would occur beyond 6 m in depth. This implies that

potential separation is possible at locations close to the ground surface. This separation

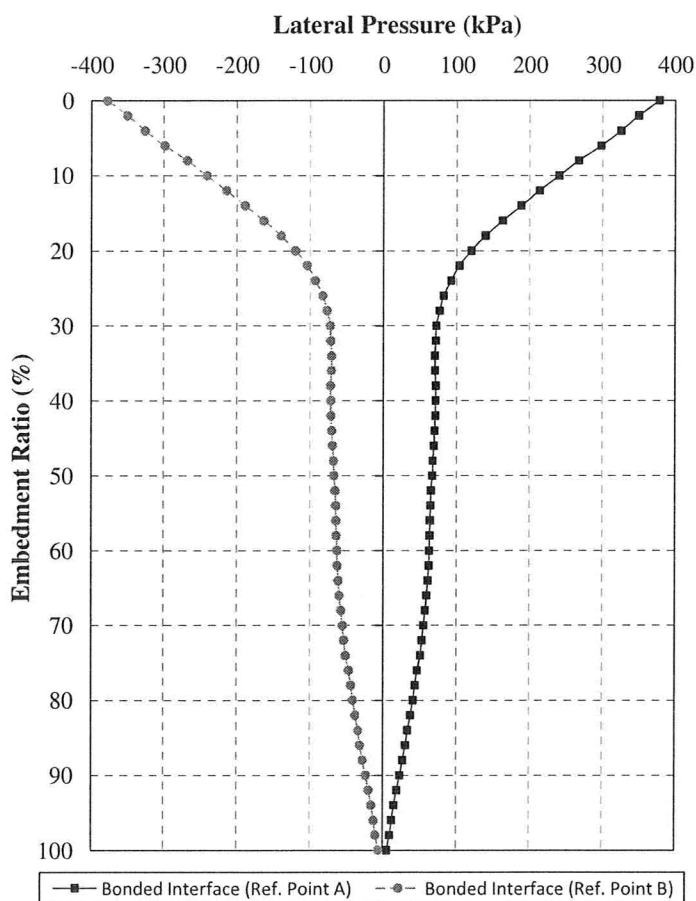significantly affects the results due to nonlinear effects.

Figure 5-5: Pressure Distribution for Bonded Interface

in Quarter Embedment

When the lateral wall displacement is concerned, the results of FEM simulation

show that the major component of the displacement is due to rigid body motion rather

than shear displacements, which produce shear loads within the foundation walls. At 9.02

second, the total wall displacement at the ground surface is about 0.78 mm. The

corresponding shear displacement is about 0.05 mm, which is about 6 percent of the total

displacement and is negligible.

(b) Half Embedment

A seismic analysis is performed for the case with half embedment (i.e.,

embedment depth is half of the wall height). The time history for lateral pressures at the

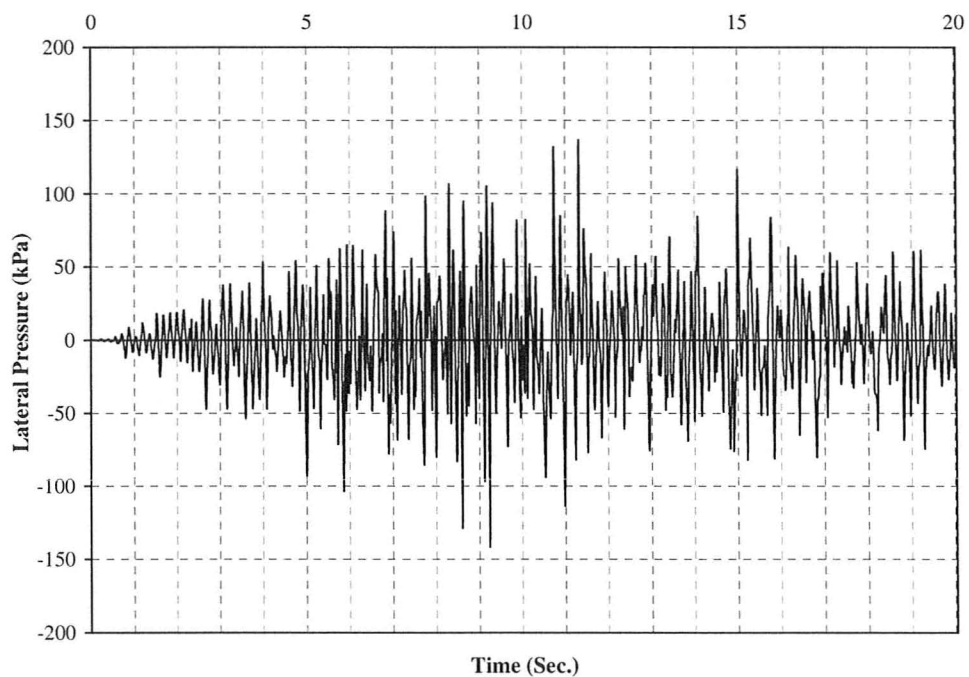reference Point A location is plotted in Figure 5-6. The plot is cut off at 20 second.

Figure 5-6: Pressure Time History at Point A for Bonded Interface for

Half Embedment

As shown in Figure 5-6, the two highest values of soil pressure are found at 9.24

second and 11.32 second. The associated peak stresses equal to -149.69 kPa and 141.38

kPa, respectively. These peak pressures are much lower than the ones determined for the quarter embedment case. This indicates that the inertial effect is dramatically reduced with increased embedded depths. Similarly, the peak pressures are found after the ground acceleration of motion are increased to 0.3 g. At this moment, the acceleration at the roof reaches the maximum value of 0.43 g, which is about half of what is obtained in the case of quarter embedment. This significant reduction in the acceleration of structural response is due to the change in structural natural frequencies, which is induced by the stiffness increase associated with the increase in embedment. With reduced projection heights, the frequencies of structural system are becoming too high to be excited by the seismic ground motion.

For the purpose of comparison, the distribution of earth pressure along the depth at the time of 11.32 second is presented in Figure 5-7. At this moment, a high pressure zone is found near ground surface area, approximately top 10% of embedment. Within the high compression zone at Point B side, the earth pressure decrease quickly from the highest value of -140 kPa at the ground surface to about -10 kPa. The earth pressure in the middle part of the wall (approximately 30% to 80% embedment) is rather uniformly distributed, with the average value being about 10 kPa. This earth pressure distribution is quite different from the results for the quarter embedment case in which the earth pressure is always in compression at Point B side. It should be noted the earth pressure distribution profile in the half embedment case is similar to that for deep pile foundations. Moreover, the positive pressures would not occur and separation at the interface of soil and structure

would not be an issue for seismic inputs with the peak ground acceleration (PGA) less than 0.3 g.
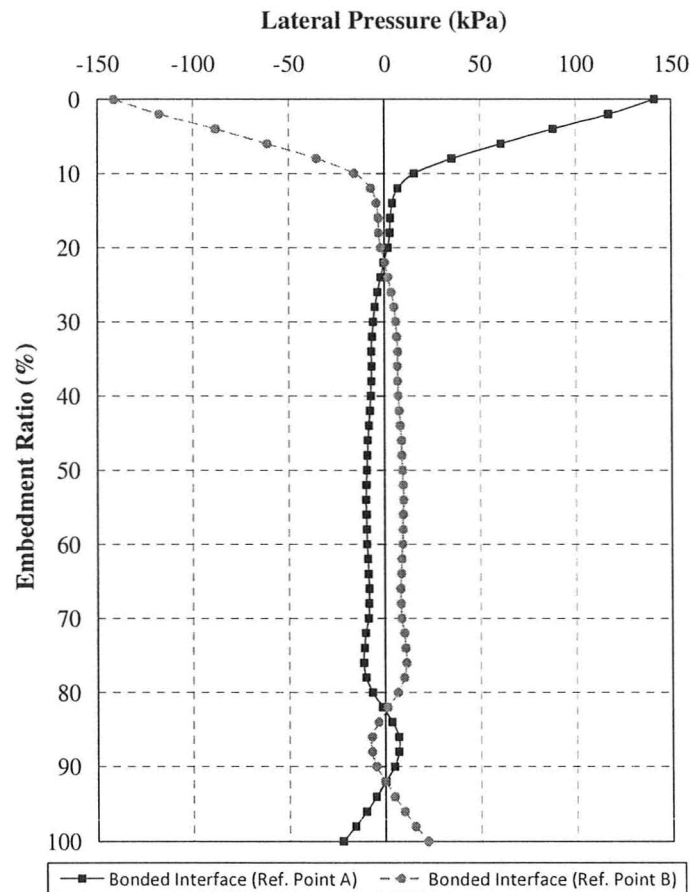

Figure 5-7: Pressure Distribution for Bonded Interface

in Half Embedment

Similar to the case of quarter embedment, the displacement of the foundation walls for the half embedment case is mainly due to rigid body motion rather than shear displacements, which produce shear loads within the foundation walls. The maximum displacement of the structure at ground surface at 11.32 second is about 1.5mm. The

corresponding shear displacement is only about 0.15 mm, which is 10 percent of total displacement. The maximum displacement at the reference point in this case is almost twice of that in the quarter embedment case since the reference point elevated with increased embedment.

When comparing Figure 5-5 and Figure 5-7, one observes that the lateral pressure distributions for the two embedment cases discussed above are comparatively different. The soil pressures for the first case (i.e., quarter embedment) are primarily controlled by the inertial forces transferred from the upper structure while the kinematic interaction is primarily responsible for the deeper embedded case. Moreover, the inertial effect has a more localized influence near the ground surface and decays quickly with the increase of embedded depth. However, the kinematic effect is found having a relatively even distribution over the embedment. Also, it is noted that the inertial effect has more severe impacts on the structure than the kinematic effect, especially for heavier rigid structures. Therefore, based on the linear elastic analysis, the deep embedment is beneficial for the reduction of seismic-induced earth pressure by eliminating inertial interaction effects. This phenomenon cannot be properly captured by any simplified pseudo analysis approach.

On the other hand, with the consideration of embedment effects, several issues, which are less of interest for shallow embedded structures, may become significant for the structures with deeper embedment. These issues, including the contact interaction at the interface boundary and soil nonlinear behavior, must be reasonably addressed in an analysis in order to reasonably characterize the seismic response of the overall soil and

structural system. To evaluate the effects due to the nonlinearities, a linear-based analysis methodology should be substituted by nonlinear analysis approaches. In the following sections, the same ANSYS models were modified by assigning nonlinear characteristics into the contact interface and soil material, respectively. The associated results are discussed and assessed accordingly.

5.3.2   Analysis with Contact Interface

In this section, the analysis focuses on the assessment of bonding/debonding effects at assigned contact interface, and associated impacts on the determination of seismic-induced soil pressures. Theoretically, the seismic response with the contact interface is closer to the real situation with the consideration of SSI effects. However, from the viewpoint of application in engineering practice, the contact nonlinearity is time consuming and requires close attention with regard to defining and adjusting parameters when carrying out numerical simulations. This could lead to numerical difficulties including non-convergence and unreliable results.

In the numerical modeling presented in this section, the interface boundary is defined as a frictional contact with a friction coefficient of 0.315 and zero tension resistance. As such, potential separation and in-plane movement between the contact elements are allowed. The selected coefficient of friction corresponds to a 17.5 degree friction angle, which is typical for the interface between cohesionless backfills and concrete. The initial geostatic stresses in soil prior to seismic excitation are considered. Since the focus in section is the influence of interface properties on soil-structure

interaction, the soil media is treated as linear elastic material to facilitate comparison between the results corresponding to bonded interface (no separation or sliding on the interface) and contact interface (both separation and sliding on the interface are allowed), respectively.

(a) Quarter Embedment

Figure 5-8 presents the variations of lateral soil pressures for both contact and bonded interface conditions in 20 second time durations. The same reference point A near the ground surface is used for the following comparisons. As shown in Figure 5-8, for the case of contact interface, only compressive earth pressure is developed on the interface. This is different with the earth pressure under bonded condition when both compressive and tensile stresses were obtained at the interface. The two highest lateral pressures per contact interface model are found at 10.38 second and 10.82 second, corresponding to the compressive stresses of -918.10 kPa and -876.96 kPa, respectively. In addition, it is observed that these peak pressure values are much higher than what is calculated using linear analysis for the bonded condition as shown in Figure 5-4 and discussed in Section 5.3.1.
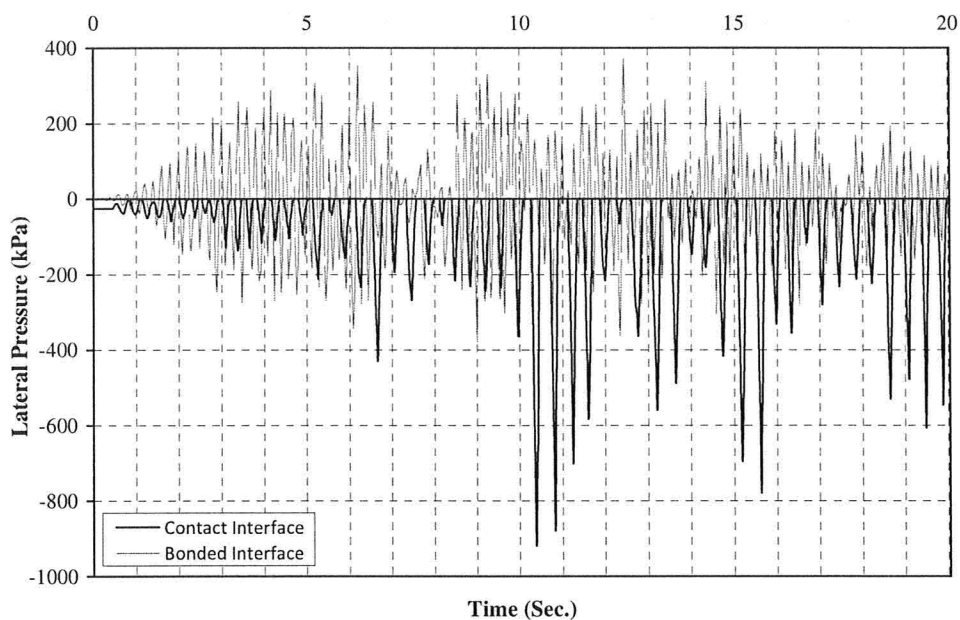
Figure 5-8: Comparison of Pressure Time Histories for Bonded and

Contact Interface for Quarter Embedment

Additionally, the time history of lateral displacement at the pre-selected Point A

near the ground surface is shown in Figure 5-9. The plotted displacements are relative

values by subtracting the structural displacement from the adjacent soil displacement. The

positive displacement indicates that separation occurs at the contact interface between the

structure and adjacent soil elements. The bonding and debonding effects at the interface

alter frequently during the period of seismic excitation. The maximum relative

displacement is found at 10.54 second. The corresponding open gap at the ground surface

is about 15.83 mm, which is small when compared to the overall building size. It is also

observed that the separation of the structure from the soil element is extended deeper

along the embedment. The same approach is used to extract the shear displacement from

the total displacement when the structure and soil are in contact. The maximum shear displacement is about 3% of the total displacement and can be considered as negligible.
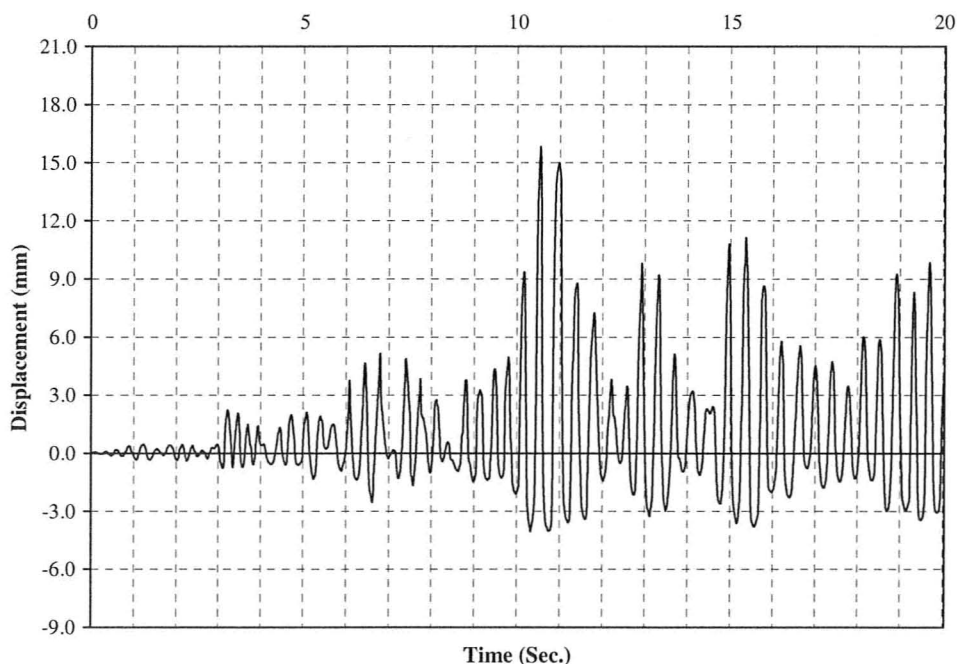

Figure 5-9: Time History of Lateral Displacement at Point A on

Contact Interface for Quarter Embedment

Figure 5-10 presents the distributions of earth pressure over embedded depth for both interface conditions. The highest pressures corresponding to 10.38 second for the contact interface and 9.02 second for the bonded interface are utilized for generic comparison. In general, high earth pressure develops in soil near the ground surface, and gradually decreases with an increase in depth. However, the magnitudes of earth pressure are very different when the interface conditions are changed. When sliding and separation are allowed on the interface (i.e., the case of contact surface), the overall pressure is

about three times the values determined from the bonded interface model in which no sliding nor separation takes place on the interface. Furthermore, the similarity in the shape of the pressure distribution curves reveals that the inertial effects are the major source to excite the seismic-induced soil pressures when the structure is shallowly embedded.
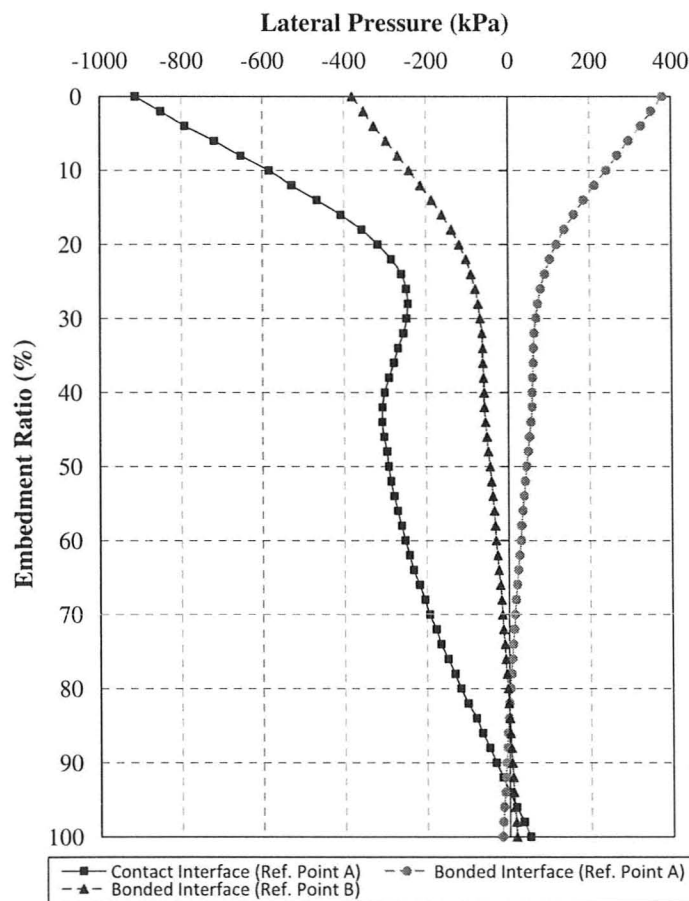

Figure 5-10: Comparison of Pressure Distribution for Bonded and Contact Interfaces for Quarter Embedment

The influence of contact conditions on the response of the roof is also identified from the results of numerical simulations. For the contact interface condition when sliding and separation are allowed, the peak response at the roof moves to the lower frequency range when compared with the bounded conditions at the interface. This phenomenon indicates that separation at the interface decreases the stiffness of the overall soil-structural system, which in turn results in increased seismic motion of the structure in the low frequency range.

(b) Half Embedment

The influence of interface conditions on seismic earth pressure is next examined at embedment depth of half wall height. Figure 5-11 shows the time history of lateral soil pressures for both interface conditions (bonded interface and contact interface) at the reference points near the ground surface during an excitation lasting 20 seconds. To be comparable, a one "g" gravity is also pre-loaded to the bonded interface model. In addition, the pressure time history at opposite Point B is used instead of Point A as the lateral pressures for contact interface are always in compression.

Two highest lateral pressures per contact interface model are found at 10.78 second and 14.78 second, corresponding to the compressive stresses of -312.39 kPa and -289.32 kPa, respectively. In the analysis using the bonded interface, two peak values of lateral stress are identified as -242.44 kPa and -248.60 kPa triggered at 10.74 second and 11.32 second, respectively. In general, it is observed that the amplitudes of seismic-induced soil pressures obtained from nonlinear analysis are much higher than what is

calculated using linear analysis for bonded interface conditions. This is caused by the stress redistribution at the soil-structure interface owing to relative displacement along the interface.
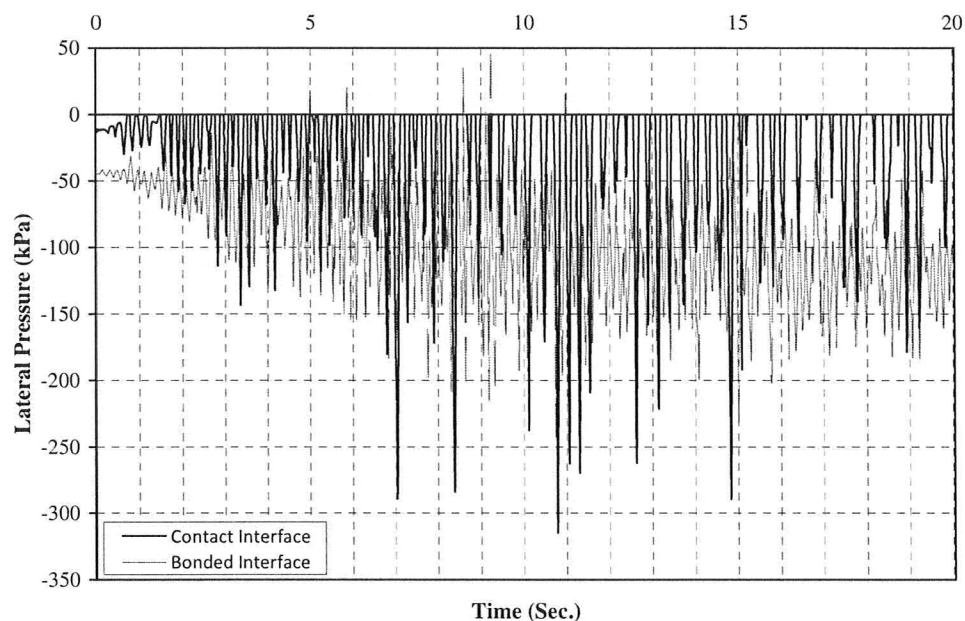

Figure 5-11: Comparison of Pressure Time Histories for Bonded and Contact Interface for Half Embedment

Similar to the discussions for the quarter embedment case, a history of lateral displacement at the pre-selected reference Point A is plotted in Figure 5-12. The plotted displacements represent the relative positions between the structure and the surrounding soil. The elements are separated at the interface when the displacement is positive, and re-bonded when the relative displacement becomes negative. The bonding and debonding effects at the interface alter frequently during the period of seismic excitation. The

maximum relative displacement is identified at 10.92 second. The corresponding open gap at the ground surface is about 12.30 mm, which is small when compared with the overall building size. It is also observed that the separation of the structure from the soil element is extensive along the embedment. The same approach is used to extract the shear displacement from the total displacement when in contact. The maximum shear displacement is less than 2% of the total displacement. The contact nonlinearity has no impact on the lateral shear displacements. This also testifies that the structure is massive and behaves as rigid-body motion. The comparison of Figure 5-9 and Figure 5-12 clearly shows that the increased embedment decreases the maximum displacement at the reference point A near the ground surface.
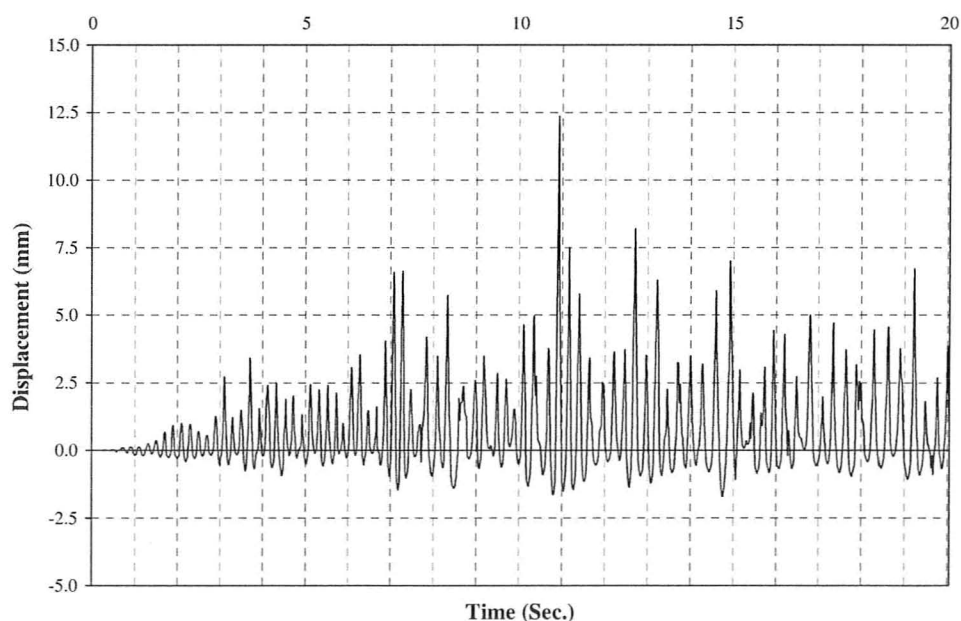

Figure 5-12: Time History of Lateral Displacement at Point A on
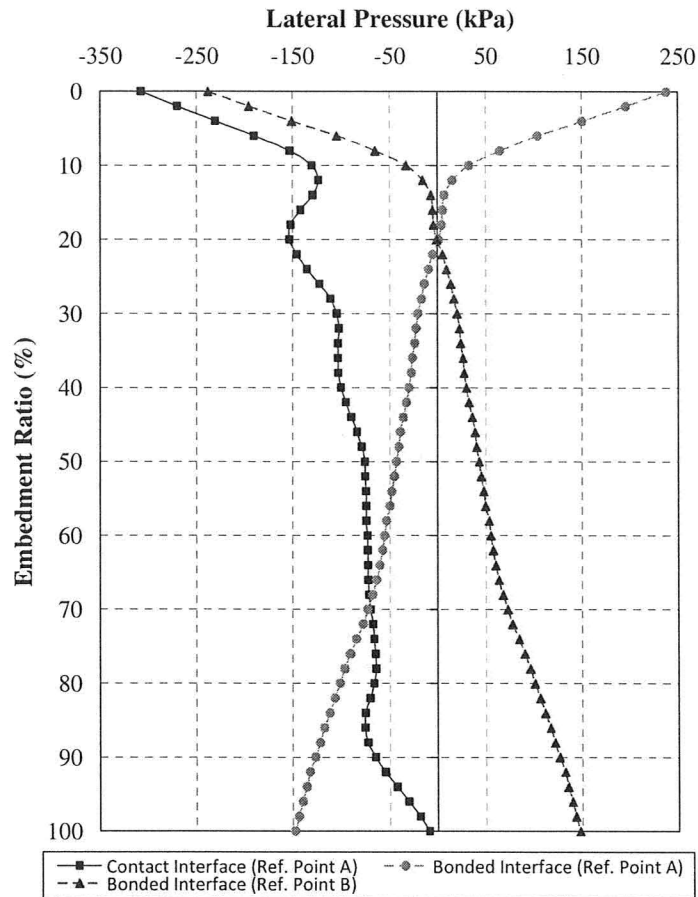
Contact Interface for Half Embedment

Figure 5-13: Comparison of Pressure Distribution for Bonded

and Contact Interfaces for Half Embedment

The pressure distributions over embedded depth are plotted for both interface conditions in Figure 5-13. The highest pressures corresponding to 10.78 second for contact interface and 11.32 second for bonded interface are utilized for comparison. It is observed from the figure that lateral pressures in middle area are relatively uniform distributed with similar configurations for both cases. However, significant deviations between these two interface conditions are noticed at locations approaching either the

ground surface or the base of the wall. It is also noted that the contact interface condition results in much higher pressures in average over the embedment. The same conclusion can be made as compared with the quarter embedment case that the inertial effects on the soil pressures are significantly decreased with the increase of embedment depth.

The impact of contact interface model on the structural responses is observed from the modeling. More specifically, the peak acceleration at the roof drifts to the lower frequency range. This phenomenon indicates that the separations at the interface decrease the stiffness of the overall soil-structural system. In addition, it is noticed that the structural response is significantly amplified, even stronger than that for shallow embedment. This observation is quite different with the original expectation.

5.3.3   Involvement of Material Nonlinearity

In this section, the effects due to the material nonlinearity are addressed and analyzed for both bonded and contact interface conditions. The comparisons with the corresponding results obtained from linear elastic analysis presented in the previous sections are also provided. All discussions in this section are based on the structural models with embedment depth of half wall height (i.e., the case of half embedment). The constitutive model of soil is chosen as the extended Drucker-Prager model, with Coulomb failure criterion defines the stress states in soil at failure and all the model parameters defined in Chapter 4. The cohesion and internal friction coefficient for the soil are defined as zero and 0.7, respectively. In order to simplify the analysis process, only soil elements

at the near field zone are assigned with the nonlinear material properties without the consideration of strain hardening effects.

(a) Bonded Interface

Seismic analyses with the bonded interface condition are first carried out to investigate the effects of material nonlinearity. The histories of lateral soil pressures for both linear and nonlinear materials are presented in Figure 5-14. The pressure variations are recorded in 20 second time periods and same reference points as described in Section 5.3.2(b) are selected for pressure comparisons. To be comparable, a one "g" gravity is pre-loaded to both models with elastic or nonlinear soil material. As shown in Figure 5-14, the lateral soil stresses for both elastic and nonlinear soil are mostly located on the compression side.

Two highest lateral pressures for nonlinear soil are observed at 7.32 second and 11.10 second. The compressive stresses corresponding to the peak time are identified as -283.62 kPa and -308.50 kPa, respectively. Comparing the analysis using linear elastic soil material, the corresponding two peak values are -242.44 kPa and -248.60 kPa triggered at 10.74 second and 11.32 second, respectively. The lateral pressures obtained when using the nonlinear soil model are slightly higher, about 20% more than the pressures calculated using linear soil model. It is believed that the higher soil pressure is induced by the stress re-distribution when yielding takes place in the soil media.
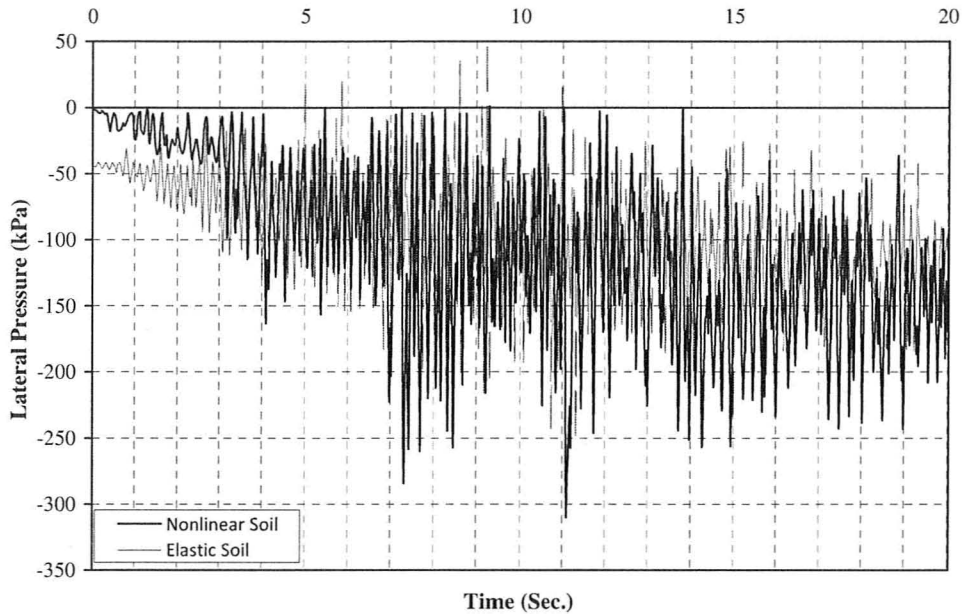
Figure 5-14: Comparison of Pressure Time Histories for Bonded

Interface with Different Soil Materials

The distributions of lateral soil pressure against embedded depth for simulations

using both linear and nonlinear soil models are plotted together in Figure 5-15. The peak

pressures at 11.32 second and 11.10 second, which correspond to linear and nonlinear

soil, respectively, are utilized for generic comparison. The magnitudes of soil pressure

are significantly amplified over the embedment when using the elasto-plasticity model. In

other words, the material nonlinearity when yielding is taken into account tends to

increase the seismic earth pressure substantially. In addition, the influence of inertia

effects becomes less important for nonlinear soil with deep embedment.
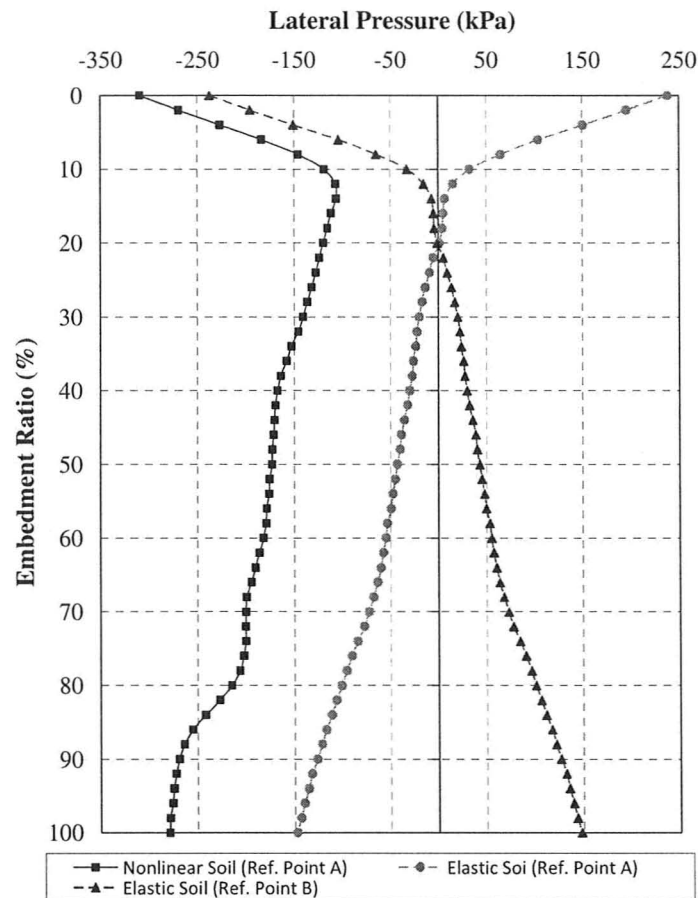
Lateral Pressure (kPa)

Figure 5-15: Comparison of Pressure Distribution for Bonded
Interface with Different Soil Materials

When comparing the effects of soil nonlinearity on structural response it is found that the response at the roof shows less sensitivity to the variation of soil properties. However, the peak acceleration at the base level is significantly amplified by the material's nonlinearity. In addition, the material's nonlinearity causes the peak amplitudes of structural motion to drift to the lower frequency range. This, in turn, is partially

responsible for the higher seismic-induced soil pressures when the nonlinearity of soil properties is taken into account.

(b) Contact Interface

The effects of soil non-linearity on seismic pressure is next examined when sliding and separation are allowed at the interface using contact interface element. The plots of pressure time history at preselected reference Point A near the ground surface for both linear and nonlinear materials with contact interfaces are presented in Figure 5-16. The time history is recorded in 20 second time durations.
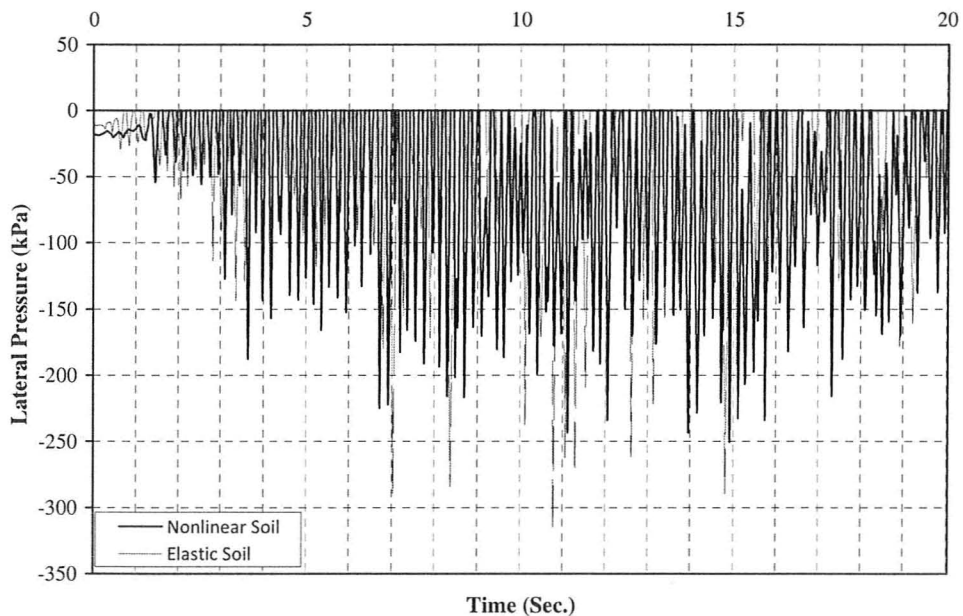

Figure 5-16: Comparison of Pressure Time Histories for Contact

Interface with Different Soil Material

As shown in Figure 5-16, for both linear and non-linear soil models, the lateral pressures are compressive at the reference point. Two highest lateral pressures for nonlinear soil are observed at 11.12 second and 14.92 second. The compressive stresses at this moment are identified as -243.19 kPa and -250.44 kPa, respectively. In the analysis using linear soil model, two peak values, which are triggered at 10.78 second and 14.78 second, respectively, are identified as -312.39 kPa and -289.32 kPa. It is noticed that the peak pressures at the selected reference point obtained from nonlinear soil are 20% lower than the pressures calculated based on linear material.

The lateral pressure distributions against embedded depth for both linear and nonlinear soil are plotted together in Figure 5-17. The peak pressures at 14.92 second and 10.78 second, which correspond to linear and nonlinear soil, respectively, are utilized for comparison. Even though the earth pressure at the ground surface is smaller for nonlinear soil, the pressure magnitudes are dramatically amplified at the depth of approximately 10% wall height. What is more important, the pressure intensity obtained from nonlinear soil is much higher than that for linear soil. Similar conclusion is made that the inertia effects on SSI are reduced with an increased embedment depth.

Based on the observation on the lateral wall displacement, it is found that the major displacement is due to rigid-body motion rather than shear displacements. It is different with the case using linear soil material, that no obvious separation is noticed from the analysis based on nonlinear material during the period of ground motion. This phenomenon is due to the material's nonlinearity, which is helpful to absorb the impact energy at the interface through the internal frictions. This also demonstrates that material

nonlinearity has significant impact on the structural dynamic analysis when considering

SSI effects.

Lateral Pressure (kPa)
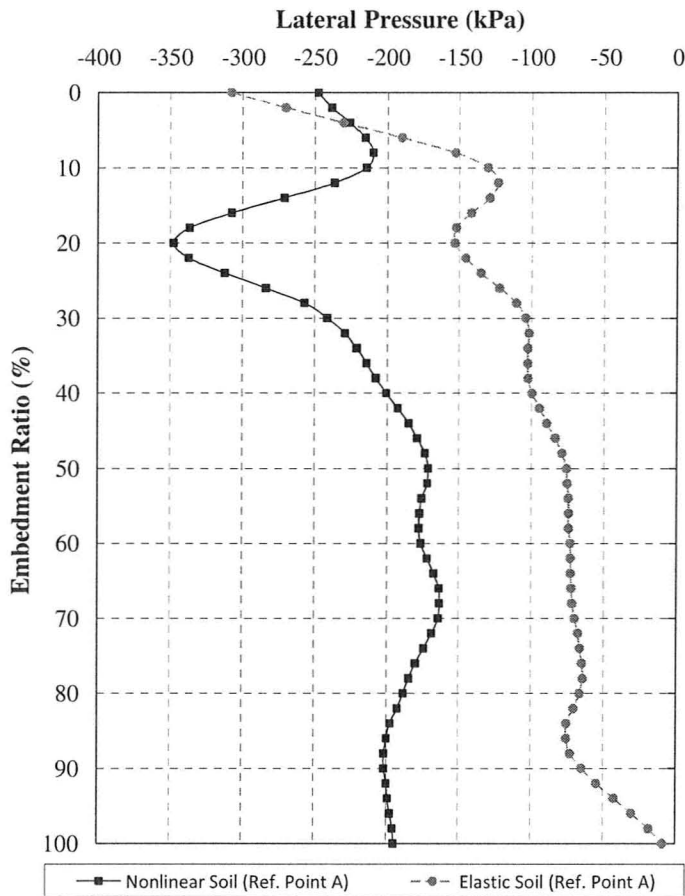
Figure 5-17: Comparison of Pressure Distribution for Contact

Interface with Different Soil Materials

The conclusion made for the bonded interface regarding the impacts on structural

response due to material change is also applicable to the contact interface condition. The

response at the roof shows less sensitivity to the variation of material properties.

However, the peak acceleration at base level is significantly amplified by the material

nonlinearity. In addition, the material nonlinearity causes the peak amplitudes to drift to the lower frequency range. This, in turn, is responsible for the higher seismic-induced soil pressure.

6 CONCLUSIONS AND RECOMMENDATIONS

Investigation on the seismic-induced soil pressures on relatively rigid structures with deep embedment was conducted in this project report. The study started with a general code review, which describes in detail the fundamental regulatory requirements applicable for deeply embedded structures relevant to seismic soil-structure interaction. A critical review was performed on traditional methodologies and available state-of-the-art approaches for the determination of the seismic earth pressure. A finite element model was established for a CANDU 6 reactor building and was utilized to investigate the seismic-induced soil pressures and associated distribution characteristics under a selected ground motion input. The results were used to evaluate and verify if current technologies can reasonably and adequately capture the seismic behaviour with the consideration to SSI effects, and to provide generic comparisons and assessments to identify how suitable and practical these recommended methods or approaches can be applied in engineering practice, especially in the nuclear engineering field.

The following conclusions are made based on the research in this report:

1. The SSI effects have significant impact on seismic-induced soil pressures. Any adjustments or changes to model parameters or input data may dramatically alter and affect the final results and conclusions. In addition, the

computation process is time consuming, especially when any nonlinear issues are involved.

2. The inertia effect and kinematic effect play significant roles in dynamic SSI analysis. The inertia interaction effect is the major source to amplify seismic-induced soil pressures when the structure is shallowly embedded. Its contribution will be gradually replaced by the kinematic effect when embedment depth is increased.

3. The inertial effect has more influence near the ground surface and decays quickly within the ground surface zone (at less than 30% of embedded depth). However, the kinematic effect is found to have a relatively even distribution over the embedment.

4. The magnitudes of seismic-induced soil pressures and associated pressure distributions are sensitive to the embedment relative to the total building height. Increased embedment tends to reduce the seismic-induced pressure by reducing the inertial interaction effects.

5. The condition of interface between the buried structure and the surrounding soil has significant effect on the seismic-induced soil pressures. Separations are noticed at the contact interface in the finite element seismic modelling. However, the size of the gap opening is not big enough to satisfy the assumption made for equivalent static analysis based on the yielding wall theory.

6. In the finite element seismic modelling, significant differences in the vertical distribution of soil pressure values are observed between the contact and bonded interface conditions. The contact interface model tends to generate much higher pressures than the bonded interface.

7. Yielding of soil during seismic loading results in noticeable changes in the soil pressure distributions over the embedment. However, the contact interface is less sensitive to the material's nonlinearity since the separation effects are significantly reduced at the contact interface.

8. For structures much stiffer than the surrounding soil, the major displacement is found due to rigid-body motion. The shear displacement along the interface is relative small and its effects are negligible.

9. Any change in embedment depth, contact interface and material properties, affect both the amplitude of peak acceleration and the corresponding frequency.

10. Linear FE analysis may not always produce conservative design when following conventional application, since the soil-structure interaction under strong ground motions is significantly affected by the nonlinear features of the system.

11. Care must be exercised when using simplified methods to calculated seismic soil pressures on underground structures. The two methods (i.e., the M-O and Koseki methods), which follow the yielding wall theory, are not

recommended as they do not properly address the dynamic soil-structure interaction under strong ground motion. In turn, both methods underestimate the lateral soil pressures.

12. The Choudhury method is not recommended for the seismic earth pressure on underground structures, even though it considered the dynamic response of soil elements. This is because the failure mechanism assumed in this method is not applicable for underground structures.

13. The methods proposed by Wood, Ostadan and Nukui do not capture the amplification and reduction effects due to the variation of the embedment which in turn affects the system's frequency. However, Wu did not specify the pressure distribution. Further study on the pressure distribution at the surface zone is still necessary.

14. The three methods proposed by Wu, Wood and Nukui, respectively, are capable of capturing the pressure amplification at the base level with the involvement of the nonlinear material properties. However, when comparing the overall thrusts, the Ostadan's method is also acceptable and may produce reasonable solutions.

15. In general, the four simplified analytical approaches following Wood, Ostadan, Nukui and Wu's methods are likely acceptable in a certain range from engineering applicable viewpoint. However, Wu's method is recommended as it has the capability to envelop most case scenarios and

presents reasonable agreement with the results obtained from detailed finite element seismic analyses.

Upon the completion of the project, it was confirmed that seismic soil structural interaction is a complex issue. The knowledge-based information and findings presented in this report can be generally used as a design reference and potentially be applicable for future design on nuclear facilities. However, there are some other issues and concerns are not properly addressed or sufficiently captured in this study. The following recommendations are outlined based on the findings and conclusions made in the project study:

1. The internal structures, including supported heavy equipment, should be incorporated into the analysis models as they are not only contribute to the mass but also significantly influence the response of overall soil-structural system;

2. The effect of interaction with adjacent structures should be properly addressed. For the CANDU 6 reactor building studied in the project, the Turbine Building and Service Building, which are usually arranged surrounding and close to the Reactor Building, should be taken into account for complete analyses;

3. The effect of partial separation encountered at the contact interface as recommended by standard ASCE 4 on soil-structure interaction and seismic earth pressure should be further investigated, with the influence of structural

geometry (e.g., rectangular or asymmetric shapes) being taken into account at the same time;

4. More effort is needed on defining the soil properties relating to its nonlinear characteristics, and reasonably assigning associated parameters into numerical analysis models to properly address the soil nonlinear issues. Those particular soil properties in concern include variable damping effects, elastic modulus, Poisson's ratio and variation of friction angles.

5. More cases with different embedment ratios should be investigated to capture the effect of embedment depth for various conditions.

6. The effects of multi-directional ground motions, both horizontal and vertical, should be examined. In addition, different ground motions shall be utilized to validate the pertinent modeling assumptions made for the analysis of SSI.

7. Laboratory and in-situ tests are necessary to verify the numerical models and to provide further insight into this specific engineering issue.

REFERENCE

[1]　　AECL, 2005, "CANDU 6 Technical Summary", 2251 Speakman Drive, Mississauga, ON, Canada.

[2]　　ANSYS Release 11.0, 2007, "Structural Analysis Guide", ANSYS Inc., 275 Technology Drive, Canonsburg, PA 15317;

[3]　　ANSYS Release 11.0, 2007, "Theory Reference for ANSYS and ANSYS Workbench", ANSYS Inc., 275 Technology Drive, Canonsburg, PA 15317.

[4]　　ASCE 4, 1998, "Seismic Analysis of Safety Related Nuclear Structures and Commentary", American Society of Civil Engineers.

[5]　　ASCE 43, 2005, "Seismic Design Criteria for Structures, Systems and Components in Nuclear Facilities", American Society of Civil Engineers.

[6]　　CAN/CSA-289.1, 2008, "General Requirements for Seismic Qualification of CANDU Nuclear Power Plants", Canadian Standards Association.

[7]　　CAN/CSA-289.2-M81, R2008, "Ground Motion Determination for Seismic Qualification of CANDU Nuclear Power Plants", Canadian Standards Association.

[8]   CAN/CSA-289.3-M81, R2008, "Design Procedure for Seismic Qualification of CANDU Nuclear Power Plants", Canadian Standards Association.

[9]   Choudhury, D. and Nimbalkar, S., 2005, "Seismic Passive Resistance by Pseudo-Dynamic Method", Geotechnique 55, No. 9.

[10]   Choudhury, D., Nimbalkar, S. and Mandal J., 2006, "Comparison of Pseudo-Static and Pseudo-Dynamic Methods for Seismic Earth Pressure on Retaining Wall", J. Ind. Geophys. Union, Vol. 10-4.

[11]   EPRI NP-2916, 1981, "Simquake II: An Multiple-Detonation Explosive Test to Simulate the Effects of Earthquake-Like Ground Motions on Nuclear Power Plant Models", Electric Power Research Institute.

[12]   EPRI NP-5513, 1987, "Large-Scale Soil-Structure Interaction", Electric Power Research Institute.

[13]   EPRI NP-5757, 1988, "Simquake III: Seismic Interaction Between Building Structures and Rock-Socketed Foundations", Electric Power Research Institute.

[14]   Eurocode 8, EN 1998, 2004, "Design of Structures for Earthquake Resistance, Part 5 – Foundations, Retaining Structures and Geotechnical Aspects", UK.

[15]   FEMA 368 & 369, 2000, "NEHRP Recommended Provisions for Seismic Regulations for New Buildings and Other Structures", Building Seismic Safety Council, Washington, D.C.

[16]   FEMA 750, 2009, "NEHRP Recommended Seismic Provisions for New Buildings and Other Structures", Building Seismic Safety Council, Washington, D.C.

[17]   Harrison, J.P., Hudson, J., 2001, "Engineering Rock Mechanics", 1st edition, Elsevier Science.

[18]   IAEA NS-G-1.6, 2003, "Safety Guide – Seismic Design and Qualification for Nuclear Power Plants", International Atomic Energy Agency, Vienna.

[19]   IAEA NS-G-3.6, 2003, "Safety Guide – Geotechnical Aspects of Site Evaluation and Foundations for Nuclear Power Plants", International Atomic Energy Agency, Vienna.

[20]   Ishihara, K., 1996, "Soil Behaviour in Earthquake Geotechnics", Oxford University Press Inc., New York.

[21]   Koseki, J., Tatsuoka, F., et al., 2007, "A Modified Procedure to Evaluate Seismic Active Earth Pressure Considering Effects of Strain Localization in Backfill Soil", University of Tokyo.

[22]   Lysmer, J., Ostadan, F. and Chin, C.C., 1999, "SASSI 2000 Theoretical Manual", Geotechnical Engineering Division, Civil Engineering Department, University of California, Berkeley, CA.

[23]   Mitchell, J.K., Soga, K., 2005, "Fundamentals of Soil Behaviour", 3rd edition, John Wiley & Sons, Inc.

[24]   Moayyedian, M., Moslem, K. and Shooshtari, A., 2008, "Proposed Dynamic Soil Pressure Diagram on Rigid Walls", IJE Transactions A, Vol. 21-3.

[25]   Mononobe, N. and Matsuo, H., 1929, "On the Determination of Earth Pressure During Earthquakes", Proceedings of World Engineering Congress, Vol. 9-176.

[26]   NBCC, "National Building Code of Canada – 2005 Edition", National Research Council Canada.

[27]   NUREG-0800, 2007, "Standard Review Plan for the Review of Safety Analysis Reports for Nuclear Power Plants: LWR Edition", US NRC.

[28]   Nukui, Y., Inagaki, Y. and Ohmiya, Y., 1989, "Fundamental Characteristics and Simplified Evaluation Method of Dynamic Earth Pressure", 10th International Conference on Structural Mechanics in Reactor Technology, Anaheim, CA.

[29]   Okabe, S., 1926, "General Theory of Earth Pressure", Journal of Japanese Society of Civil Engineers, Vol. 12-1.

[30]   Ohara, S., Maehara, H. and Nagata, H., 1970, "On Active Earth Pressure During Earthquake", Tsuchi-to-Kiso, JSSMFE, Vol. 18, No. 2.

[31]   Ostadan, F., 2005, "Seismic Soil Pressure for Building Walls – An Updated Approach", Bechtel Technology Journal.

[32] Park, Y. J. and Hofmayer, C. H., 1994, "Technical Guidelines for Aseismic Design of Nuclear Power Plants: Translation of JEAG 4601 – 1987", US Nuclear Regulatory Commission.

[33] Park, Y. J., Hofmayer, C. H. and Costello, J. F., 1994, "Understanding Seismic Design Criteria for Japanese Nuclear Power Plants", US Department of Energy's.

[34] Richards, R and Elms, D.G., 1979, "Seismic Behavior of Gravity Retaining Walls", ASCE, Journal of Geotechnical Engineering, Vol. 105, No. GR4.

[35] Roesset, J. M., 1989, "Perspectives on Soil Structure Interaction Analysis", Proceedings of EPRI/NRC/TPC Workshop on Seismic Soil-Structure Analysis, Lotung, Taiwan.

[36] Romanel, C. et al., 1993, "Analysis of Deeply Embedded Structures in a Layered Half-Space", Proceedings of the 12th International Conference on Offshore Mechanics and Arctic Engineering, ASME, Glasgow, Scotland.

[37] Seed, H.B. and Idriss, I.M., 1970, "Soil Moduli and Damping Factors for Dynamic Response Analyses", Report No. EERC 70-10, University of California, Earthquake Engineering Research Center, Berkeley, California, USA.

[38] Seed, H.B. and Whitman, R.V., 1970, "Design of Earth Retaining Structures for Seismic Loads", ASCE Specialty Conference on Lateral Stresses in the Ground and Design of Earth Retaining Structures, Cornell University, Ithaca, New York.

[39]   Steedman, R.S. and Zeng, X., 1990, "The Influence of Phase on the Calculation of Pseudo-Static Earth Pressure on a Retaining Wall", Geotechnique, 40 (1).

[40]   Tajimi, H., 1985, "Soil-Structure Dynamic Interaction", in Japanese.

[41]   Tseng, W.S. and Hadjian, A.H., 1991, "Guideline for Soil-Structure Interaction Analysis", NP-7395 Final Report, Bechtel Group Inc., San Francisco, California.

[42]   Vanmarcke, E.H., 1976, "SIMQKE – A Program for Artificial Motion Generation, User's Manual and Documentation", Dept. of Civil Engineering, Massachusetts Institute of Technology (MIT).

[43]   Veletsos, A and Younan, A.H., 1994, "Dynamic Soil Pressure on Rigid Vertical Walls," Earthquake Engineering and Soil Dynamics, Vol. 23.

[44]   Verruijt, A., 2010, "Soil Mechanics", Delft University of Technology, Netherlands.

[45]   Wood, J.H., 1973, "Earthquake Induced Soil Pressures on Structures", PhD Thesis, California Institute of Technology, Pasadena, CA.

[46]   Wolf, J. P., 1985, "Dynamic Soil-Structure Interaction", Prentice-Hall, Inc., Englewood Cliffs, New Jersey.

[47]   Wolf, J. P., Song, C, 1996, "Finite-Element Modeling of Unbounded Media", John Wiley & Sons, Inc.

[48]   Wu, G. and Finn, W.D.L., 1999, "Seismic Lateral Pressures for Design of Rigid Walls", Canadian Geotechnical Journal, Vol. 36-3.

[49]   Xu, J., Miller, C., Costantino, C. and Hofmayer, C., 2005, "Evaluation of Seismic Induced Wall Pressures for Deeply Embedded NPP Structures", 18th International Conference on Structural Mechanics in Reactor Technology, Beijing, China.